Presented at the Third Symposium on
the Physics and Chemistry of Fission,
Rochester, New York, August 13-17, 1973

RECEIVED
LAWRENCE
RADIATION LABORATORY

AUG 8 1973

LIBRARY AND
DOCUMENTS SECTION

LBL-1914
c.2

FISSION PROBABILITIES IN LIGHTER NUCLEI. A THEORETICAL AND EXPERIMENTAL INVESTIGATION OF THE SHELL AND PAIRING EFFECTS IN FISSIONING NUCLEI

L. G. Moretto

July 1973

Prepared for the U. S. Atomic Energy Commission
under Contract W-7405-ENG-48

TWO-WEEK LOAN COPY

This is a Library Circulating Copy
which may be borrowed for two weeks.
For a personal retention copy, call
Tech. Info. Division, Ext. 5545

LAWRENCE BERKELEY LABORATORY
UNIVERSITY OF CALIFORNIA
BERKELEY

LBL-1914
c.2

DISCLAIMER

This document was prepared as an account of work sponsored by the United States Government. While this document is believed to contain correct information, neither the United States Government nor any agency thereof, nor the Regents of the University of California, nor any of their employees, makes any warranty, express or implied, or assumes any legal responsibility for the accuracy, completeness, or usefulness of any information, apparatus, product, or process disclosed, or represents that its use would not infringe privately owned rights. Reference herein to any specific commercial product, process, or service by its trade name, trademark, manufacturer, or otherwise, does not necessarily constitute or imply its endorsement, recommendation, or favoring by the United States Government or any agency thereof, or the Regents of the University of California. The views and opinions of authors expressed herein do not necessarily state or reflect those of the United States Government or any agency thereof or the Regents of the University of California.

FISSION PROBABILITIES IN LIGHTER NUCLEI. A THEORETICAL AND EXPERIMENTAL INVESTIGATION OF THE SHELL AND PAIRING EFFECTS IN FISSIONING NUCLEI*

L. G. Moretto

Department of Chemistry and
Lawrence Berkeley Laboratory
University of California
Berkeley, California 94720

July 1973

ABSTRACT

The general features of the fission probabilities are reviewed in the light of the modern developments on the statistical properties of nuclei. The general thermodynamical aspects of the fission probabilities are first discussed without relying on any specific nuclear model. The effects of the shell structure and of the collective degrees of freedom on the saddle-point and ground state phase space volume are then considered. A general method to include the effect of shells and pairing in the fission probability calculation is illustrated. The disappearance of the shell and pairing effects with increasing excitation energy and its influence on the fission probabilities is exemplified by means of a calculation performed on superheavy elements. The experimental data available in nuclei in the Pb region and lighter nuclei are discussed in detail and an analysis based upon the present knowledge of shell and pairing effects is performed. It is found that the experimental evidence on shell effects in these data are accounted for satisfactorily by including the Nilsson model and the BCS Hamiltonian in the calculation. A reliable set

*Third Symposium on the Physics and Chemistry of Fission, Rochester, New York, August 13-17, 1973.

of fission barriers is obtained and the liquid drop model predictions are tested. The saddle point single particle level densities which are also obtained in the analysis show the expected A dependence and their magnitude, about 8% larger than the corresponding ground state quantity, seems to be due to an increase in the nuclear surface at the saddle point.

INTRODUCTION

Already in 1939, immediately after the discovery of fission, it became apparent that the fission decay rate is controlled by a rather impenetrable potential energy barrier.[1] The existence of this barrier found its natural explanation in the liquid drop model,[2] which was to become the leading model in the fission process.

At the same time the theory of the chemical reaction rates, based upon the existence of an activated complex (or transition state), was employed to estimate the fission decay rate.[1]

An equivalently good theoretical knowledge of the neutron and radiation decay widths,[3] associated with the expected exponential rise of the level density with excitation energy led to a very early theoretical understanding of the fission probabilities.[1,4]

The first data on fission probabilities to become available was in the actinide region.[5] In these elements the fission barrier height and the neutron binding energy are very close and the resulting fission probability at energies above the barrier varies very slowly with energy.

The observations of fission cross sections rapidly rising with energy in lighter elements, for which the fission barrier is much larger than the neutron binding energy, prompted a new theoretical and experimental effort which on one hand led to more accurate theoretical expressions for the fission probabilities on the basis of the uniform model,[5,6] on the other produced an increasing wealth of experimental data on lighter elements[7-18] and at energies very close to the fission barrier.[13,14,16-18] One should explicitly mention the pioneering work by Huizenga *et al.*[13], the determination of the fission barrier of ^{201}Tl by

Burnett et al.[14] and the work by the Berkeley group.[16-18] The greatest part of the available cross section data which could be included in two figures is shown in Figs. 1 and 2.

The analysis of the data on the basis of the early theories successfully accounted for the rapidly rising fission cross sections and produced reliable fission barriers. To a large extent the barrier determinations have been and still are the most relevant results obtained in the analysis of fission probabilities, for their contribution to the understanding of the potential energies surfaces and of the liquid drop model parameters. Clear indications of the shortcomings of the uniform model, and of the necessity for more accurate models to be used in the evaluation of the level densities were also apparent.[16] The data could be fitted only over a short energy range, and the level density parameters extracted from the data fitting showed marked fluctuations attributable to the shell structure.

More recently, refined level densities, generated on the basis of the shell model[19-22] and of the pairing Hamiltonian,[23-30] have become available and have made it possible to account for the shell structure effects in a nearly quantitative way. These new level densities have proven to be remarkably successful in the analysis of the fission cross sections of the lighter elements[31,32] as well as in the analysis of the fission and isomer formation cross sections in the actinides.[33,34] A similar study has also been extended to the superheavy nuclei in order to investigate their stability towards fission at the compound nucleus stage.[35-37]

In the present paper all of the above developments are presented to various extents. In Sec. 1 the general features of the fission probability theory are outlined, and the limiting behavior of the fission probability at

high energies is derived. Furthermore, the insensitivity of this quantity to the fine details of the Hamiltonian is pointed out. In Sec. 2 the results obtained by using the uniform model in the analysis of the lighter element data are presented and the shortcomings of such a model are discussed. In Sec. 3 some recent and new aspects of the problem are treated, like the relevance of the collective degrees of freedom to the fission decay width, and the way in which shell and pairing effects can be included in the calculation of the fission probabilities. The latter point is illustrated with the calculation of the fission probabilities in superheavy elements. In Sec. 4 the available experimental data for lighter elements are critically analyzed and the results of the fitting procedure are discussed.

As a last comment the data available for lighter elements have been given special attention in this paper. Very important work has been and is being performed in the actinide region and will appear in other contributions to this conference.

Sec. I. THE FISSION AND NEUTRON WIDTHS: STANDARD FORMULAE AND LIMITING BEHAVIOR

In this section an effort is made to derive various limiting forms of the fission probability without resorting to any detailed nuclear model. It can be shown that the physical features of the system can be summarized in terms of simple thermodynamical quantities, like the temperature which are rather independent of the nuclear structure details and vary slowly with energy.

A nucleus, whose excitation energy is equal or larger than the fission barrier, is expected to move randomly in a restricted region of configuration space (the compound nucleus region) until, by chance, it finds access to the potential energy saddle which leads to a new, almost unrestricted region of configuration space (the region of the forming fission fragments). The decay probability is equal to the number of systems per unit time overcoming the barrier divided by the number of systems remaining in the compound nucleus region. If the access to the barrier is random, the population of the compound nucleus region and that of the saddle region can be taken to be proportional to the respective phase-space volumes. The randomness assumption should be met if the total decay width of the compound nucleus is small, namely, if its lifetime is long.

Under these conditions the fission decay width can be written as:

$$\Gamma_F = \frac{1}{2\pi\rho(E)} \int_0^E \rho_S(x)\, P(E - B_F - x)dx \qquad (1)$$

where $\rho(E)$ is the level density of the compound nucleus at the excitation energy E, B_F is the fission barrier height, $\rho_S(x)$ is the saddle point level density at the excitation energy x and $P(E - B_F - x)$ is the quantum-mechanical probability of penetrating the barrier. This last quantity, for a parabolic barrier takes the form:[36]

$$P = \frac{1}{1 + \exp - \frac{2\pi(E - B_F - x)}{\hbar\omega}}$$ where $\hbar\omega$ is the phonon

energy associated with the parabolic potential, called barrier penetrability coefficient. An important feature of the level density $\rho_S(x)$ is that it refers to all the collective and intrinsic modes of the system with the exclusion of the fission mode.

The neutron decay width can be evaluated along similar lines and takes the form:

$$\Gamma_N = \frac{1}{2\pi\rho(E)} \frac{4m_N}{\pi\hbar^2} \int_0^{E-B_N} \sigma_{inv} \rho_R(x) (E - B_N - x)dx \tag{2}$$

where m_N is the neutron mass, B_N is the neutron binding energy, σ_{inv} is the cross section associated with the inverse process and $\rho_R(x)$ is the level density of the residual nucleus.

One can take advantage of the strong energy dependence of the level densities and evaluate both expressions by suitably expanding the integrand about the upper limit of integration. The following expression is obtained for the fission width:

$$\Gamma_F = \frac{1}{2\pi\rho(E)} \frac{1}{D_S} \rho_S(E - B_F) \quad , \tag{3}$$

where the penetrability P has been taken equal to one above, and zero below the barrier and

$$D_S = \left. \frac{d \ln \rho_S(x)}{dx} \right|_{x=E-B_F}$$

For the neutron width one obtains:

$$\Gamma_N = \frac{1}{2\pi\rho(E)} \sigma_{inv} \frac{4m_N}{\pi\hbar^2} \frac{1}{D_R^2} \rho_R(E - B_N) \tag{4}$$

where the inverse cross section has been assumed to be independent of energy and $D_R = \left. \frac{d \ln \rho_R(x)}{dx} \right|_{x=E-B_N}$. Recalling that in statistical mechanics $\frac{d \ln \rho}{dx} = \frac{dS}{dE} = \frac{1}{T}$, the quantities $1/D_S$ and $1/D_R$ assume the meaning of the saddle point and residual nucleus temperatures T_S and T_N, respectively.

The ratio $\frac{\Gamma_F}{\Gamma_N}$ can then be expressed in the following simple form:

$$\frac{\Gamma_F}{\Gamma_N} = \frac{\pi\hbar^2}{4\sigma_{inv} m_N} \frac{T_S}{T_R^2} \frac{\rho_S(E - B_F)}{\rho_R(E - B_N)} \tag{5}$$

This approximation is accurate even at rather low excitation energies. The above equation can be further simplified by expanding both level densities about the energy $E - \overline{B}$ where $\overline{B}$ is intermediate between B_F and B_N:

$$\frac{\Gamma_F}{\Gamma_N} = \frac{\pi\hbar^2}{4\sigma_{inv} m_N} \frac{T_S}{T_R^2} \frac{\rho_S(E - \overline{B})}{\rho_R(E - \overline{B})} \exp\left(\frac{B_N}{T_R'} - \frac{B_F}{T_S'}\right) \tag{6}$$

where T_R' and T_S' are the effective temperatures in the residual nucleus and at the saddle at an excitation energy $E - \overline{B}$. Such an approximation becomes

better the closer B_F is to B_N and the larger is the excitation energy E. In fact, as the excitation energy increases, the temperatures T_S, T_R, T_S', T_R' tend to a unique value T. One can also assume that the two level densities $\rho_S(E - \overline{B})$ and $\rho_R(E - \overline{B})$ are equal, which may be a good approximation in absence of shell and pairing effects. Assigning to the inverse cross section its geometric value one obtains:

$$\frac{\Gamma_F}{\Gamma_N} = 5.25\ A^{-2/3}\ T^{-1}\ \exp\left(\frac{B_N - B_F}{T}\right) \tag{7}$$

Equation (7) and to large extent Eq. (5) and Eq. (6) are remarkable for their almost total lack of physical details aside from the neutron binding energy and the fission barrier height. One does not even need to assume any special form for the level densities. This is an aspect of statistical theories which has both good and bad features and which, while easily and simply interpreting experimental data, yield information very reluctantly on the detailed Hamiltonian of the system. By means of Eq. (7) the asymptotic behavior of Γ_F/Γ_N can be estimated. For $(B_N - B_R) \geqslant 0$ the function is monotonically decreasing and eventually tends to zero as $\frac{1}{T}$. For $(B_N - B_F) < 0$ the function has a maximum at $T = B_F - B_N$ and then it decreases again, tending to zero at large temperatures like $\frac{1}{T}$. The dominance of the neutron decay over the fission decay at high energies is a consequence of the phase-space volumes available to the two modes of decay when energy restrictions become irrelevant as in the case of large temperatures. Everything being equal, three unbound modes are available for the emission of neutrons (the three cartesian coordinates of the free neutron) while only one unbound mode is available for fission (the saddle

point fission mode). It is also quite interesting to notice that Γ_F/Γ_N tends to zero as the mass number of the system tends to infinity. The $A^{-2/3}$ dependence of $\frac{\Gamma_F}{\Gamma_N}$ is signifying the increasing "surface area" from which neutrons can evaporate.

The formalism described so far can be generalized to include the effect of angular momentum. The presence of angular momentum implies that a certain amount of energy is present in form of rotational energy, and it is not available to excite the internal degrees of freedom. Therefore, Eq. (5) can be modified as follows:

$$\frac{\Gamma_F}{\Gamma_N} = \frac{\pi\hbar^2}{4\sigma_{inv}\, m_N} \frac{T_S}{T_R^{\,2}} \frac{\rho_S(E - B_F - E_S^I)}{\rho_R(E - B_N - E_R^{I'})} \tag{8}$$

where $E_S^I = \frac{\hbar^2 I^2}{2\mathfrak{J}_S}$ is the rotational energy at the saddle point; $E_R^I = \frac{\hbar^2 I'^2}{2\mathfrak{J}_R}$ is the rotational energy in the residual nucleus after neutron emission; I is the total angular momentum; $I'^2 = I^2 + \overline{\ell^2}$ and $\overline{\ell^2}$ is the average angular momentum associated with the emitted neutrons. (The approximate way in which the angular momentum is handled in Γ_N is well justified at moderate excitation energies.[37]) The two moments of inertia $\mathfrak{J}_R$ and $\mathfrak{J}_S$ depend in general upon both the excitation energy and the angular momentum. A very complete study of the equilibrium shapes of liquid drop nuclei in the ground state and at the saddle point has been performed by Cohen, Plasil and Swiatecki[38,40] and by Cohen and Swiatecki.[39] For relatively small angular momenta one can assume the zero angular momentum shapes for the evaluation of the rotational energies. Rewriting Eq. (7) on this basis one obtains:

$$\frac{\Gamma_F}{\Gamma_N} = 5.25\ A^{-2/3}\ T^{-1}\ \exp\ \frac{\{B_N - B_F - (E_R^{I'} - E_S^{I})\}}{T} \tag{9}$$

This expression indicates that the presence of angular momentum decreases the effective fission barrier by an amount $(E_R^{I'} - E_S^{I})$ which is always positive since $\mathfrak{J}_S > \mathfrak{J}_R$. At larger angular momenta the fission barrier itself is decreasing due to a change in the saddle point deformation, thus increasing even more the fissionability of the nucleus.

Sec. II. PRELIMINARY DATA ANALYSIS WITH SIMPLE LEVEL DENSITY EXPRESSIONS

The formalism presented in the previous section requires the use of specific level density expressions both in Γ_F and in Γ_N. It is mainly in these quantities that all the physical information concerning the nucleus at the saddle point and the residual nucleus after neutron emission is contained.[41]

Until very recently, the statistical properties of nuclei have been described on the basis of the uniform model.[42,43] In this model the nucleus is represented as a system of non-interacting fermions occupying equidistant non-degenerate single-particle levels. Although this picture contains little physics beyond the Pauli principle, still its application to problems like the present one has had a reasonable success.

The expression for the uniform model level density is:

$$\rho(E) = \frac{\sqrt{\pi}}{12} \frac{e^{2\sqrt{aE}}}{a^{1/4} E^{5/4}} \tag{10}$$

where E is the excitation energy of the system and a is the level density parameter, which is related to the single-particle level density g by the expression:

$$a = \frac{\pi^2}{6} g$$

The level density parameter a is expected to vary in proportion to the mass number of the nucleus: $a = \frac{A}{K}$, where K is a constant whose value is estimated to be around 8 or 9.[44] Explicit expressions for the quantity Γ_F/Γ_N have been given by Huizenga and Vandenbosch[6] on the basis of the uniform model. In these calculations only the leading factor of Eq. (10) has been used, namely:

$$\rho(E) \propto e^{2\sqrt{aE}} \tag{11}$$

Almost all of the experimental data available at present have been analyzed in terms of the uniform model level density.[13,14,16,17] Here we shall report the overall conclusions of such an analysis applied to lighter nuclei, without any critical comment on the data themselves, which will be delayed until Sec. 4.

The free parameters typically employed in this data fitting procedure are: the fission barrier B_F; the penetrability coefficient $\hbar\omega$; and Γ_F and Γ_N level density parameters a_F and a_N. The quantities which the fitting procedure can most solidly establish are the fission barrier B_F and the ratio $\frac{a_F}{a_N}$.

The experimental Γ_F/Γ_N quantities have been readily fitted up to 20 MeV above the fission barrier. In this energy range some of the experimental data cover more than six order of magnitude. The fission barriers have proven to be rather insensitive to small variations in the other parameters. The individual values of a_F and a_N turn out to be quite uncertain, while their ratio tends to remain constant. Two difficulties immediately arise. The first is related to the a_F/a_N ratio which appears to be close to unity in nuclei far away from the shell region and as high as 1.5 for nuclei in close vicinity to ^{208}Pb. The second difficulty is the inability to fit the data in a larger energy interval for the latter kind of nuclei. Because of the large ratio of $\frac{a_F}{a_N}$ necessary to fit the low energy data, the fission probability increases much too rapidly with energy to fit the higher energy data. In other words, it appears that for this kind of nuclei the effective a_F/a_N ratio varies smoothly from a rather large value close to the fission barrier to a value close to unity at higher energies. At the same time it is

found out that the experimental fission barriers can be decomposed in two parts: a smooth liquid drop quantity and a ground state shell effect which measures the deviation between the experimental ground state mass and its liquid drop prediction. This shell correction is at a maximum in the Pb region and has the effect of producing a strong local increase in the fission barriers. The mounting evidence indicates that the anomalously high fission barriers in the Pb region and the corresponding large ratio of a_F/a_N are two facets of the same physical fact, namely the small single particle level density at the Fermi surface of the spherical nuclei due to the double shell closure in ^{208}Pb. At the same time the data are strongly suggesting that the effect of the shells is disappearing rather rapidly with increasing excitation energy.

An overall view of the studies illustrated above allows one to reach the following conclusions.

a) The statistical formalism is potentially able to fit the experimental fission probabilities over many orders of magnitude;

b) Fission barrier heights can be extracted rather safely from the analysis of low energy cross sections;

c) The obtained fission barriers so obtained can be decomposed into a smooth liquid drop component and the ground state shell correction;

d) The uniform model is inadequate in justifying the widely varying ratio of a_F/a_N and in reproducing the fission probabilities over a large energy range.

Sec. III. MODERN PROBLEMS IN THE EVALUATION OF THE PHASE SPACE VOLUMES RELEVANT TO THE FISSION PROBABILITIES

The use of the uniform model in the evaluation of the fission probabilities does not allow one to interprete the experimental data satisfactorily. Rather serious problems are met in the attempt to evaluate the detailed form of the phase space volume associated with the fission and neutron decay. Some of these problems can be solved, others have not yet been considered in depth. In the present section some of these problems will be considered. In the first part, the coupling between the collective and the internal degrees of freedom will be studied especially insofar as the fission width is concerned. In the second part the simpler but better understood problem of the inclusion of shell and pairing effects in the formalism will be discussed. In the third part some examples of calculation of the fission probabilities of superheavy nuclei will be shown to illustrate the disappearence of the shell effects with excitation energy.

Relevance of the Collective Degrees of Freedom in Γ_F. The peculiar collective nature of the fission process raises serious questions regarding the contribution of the collective degrees of freedom to the shape and volume of the phase space which controls the fission decay widths. This is particularly important when one needs to consider the fission width as a differential in the various saddle point collective coordinates and momenta. In order to explore to what extent such collective degrees of freedom affect the fission widths, let us express them explicitly in Eq. (1). The introduction of n bound normal modes, besides the fission mode, leads to the following expression:

$$\Gamma_F = \frac{1}{2\pi\rho(E)} \int d\varepsilon \int \Pi \frac{dx_i \, dp_i}{h^n} \rho_S'(E - B_F - \varepsilon - \Sigma\{\tfrac{1}{2} a_i x_i^2 + p_i^2/2m_i\}) \tag{12}$$

where ε is the kinetic energy along the fission coordinate; x_i and p_i are the saddle point normal coordinates and momenta; a_i and m_i are the stiffnesses and the inertias associated with the same normal modes; the quantity ρ_S' is the level density due to the intrinsic degrees of freedom; the integration limits in the multiple integral are taken in such a way as to conserve energy. By profiting again from the strong energy dependence of ρ_S' and by setting $\frac{d \ln \rho_S'(x)}{dx} = \frac{1}{T}$ we can rewrite Eq. (12) as follows:

$$\Gamma_F = \frac{1}{2\pi\rho(E)} \rho_S'(E - B_F) \frac{1}{h^n} \int_0^{\infty} e^{-\varepsilon/T} d\varepsilon \int_{-\infty}^{+\infty} e^{-\Sigma p_i^2/2m_i T} \Pi dp_i \int_{-\infty}^{+\infty} e^{-\Sigma \frac{1}{2} a_i x_i^2/T} \Pi dx_i \tag{13}$$

In this expression the energy is not rigorously conserved: in fact such an expression is well known in statistical mechanics as the canonical expansion where the temperature, instead of the energy, characterizes the system. In this case, the many internal degrees of freedom of the nucleus are acting as a thermostat with which the collective degrees of freedom are at equilibrium.

The integration of Eq. (13) can be easily performed:

$$\Gamma_F = \frac{1}{2\pi\rho(E)} \rho_S'(E - B_F)\, T \boxed{\left(\frac{2\pi T}{h}\right)^n \Pi \sqrt{\frac{m_i}{a_i}}} \tag{14}$$

where the quantity in the box represents the phase space volume contribution of the collective degrees of freedom. This expression can be compared with Eq. (3). The two expressions are identical if one sets,

$$\rho_S(E - B_F) = \rho_S'(E - B_F) \left(\frac{2\pi T}{h}\right)^n \Pi \sqrt{\frac{m_i}{a_i}} \tag{15}$$

The above discussion leads to interesting observations regarding the validity of Eq. (3). An obvious failure of this equation occurs if one or more normal modes besides the fission mode are unbound, namely if one or more of the a_i are negative. This is predicted to occur by the liquid drop model below the Businaro-Gallone point ($x = 0.396$) where the mass asymmetry mode becomes unbound.[47] Increasing displacements away from the saddle point along this coordinate lead to a rapidly diverging integrand in Eq. (12). Under these circumstances the canonical expansion about the saddle point cannot be justified. In fact, the main contribution to the integral along the mass asymmetry coordinate comes from around the extreme mass asymmetries and not from the symmetric region around the saddle point. In this region of the fissionability parameter fission loses its identity and merges into the evaporation (spallation) reaction; the decay width calculated by Eq. (12) refers to the statistical emission of particles as a whole. As a consequence a naive analysis of "fission" cross sections for elements below Ag ($x \cong 0.4$) will indicate fission barriers smaller than those predicted by the liquid drop model. In these kind of experiments "fission" and the resulting fission barrier are defined only by the arbitrariness of the experimenter, or by the mass cut-off of the detector.

Besides the above glaring inapplicability of Eq. (3) and Eq. (14), more delicate points can be raised by the peculiar factorization of the phase space in Eq. (14) and (15). It is possible that the collective degrees of freedom are sharply defined and nearly uncoupled from the intrinsic degrees of freedom, leading to such a simple factorization of the phase space. On the other hand, the single particle degrees of freedom may be very pure, leading to a much less collective description of the system.

It is not very clear which of the two alternatives is more realistic, the second one being further plagued by the extra complication of having to define the number of collective degrees of freedom. These two extreme possibilities bring forth the problem of the microscopic nature of collective degrees of freedom in a manybody system. The collective states, borne out of very special combinations of intrinsic states, may be coupled to the remaining internal degrees of freedom to a varying extent. In the limit of complete uncoupling, the collective states have a physical existence and do play an explicit role in the form of the phase space volume at the saddle point. This phase space volume should have the form of Eq. (14) in the high temperature limit, and a more complicated form accounting for the quantum-mechanical effects at lower temperatures.[48,49] The coupling of the collective states to the intrinsic states has the effect of diluting the collective nature of the levels over the neighboring intrinsic levels. The collective aspects of the system now appear as strength functions. In classical terms, the motion along the collective coordinates becomes affected by viscosity, the largest momenta are strongly damped-out and the phase space associated with them is distorted and limited. As the collective motion becomes damped beyond criticality, the strength function loses its structure and the collective state is reabsorbed into the background of intrinsic levels. Therefore, depending on whether viscosity is large or small, the two extremes of the picture do apply. This uncertainty is not very important at high energies or when the integrated form of the decay width is considered. Instead, it is of extreme relevance when the differential form of the decay width in the coordinates and momenta of some collective coordinates is to be

used to establish the distribution of the initial conditions for the dynamical descent from the saddle to the scission point. Unfortunately, complication adds to complication since similar considerations apply for the neutron width Γ_N as well although to a somewhat smaller degree. In fact, this very modern problem directly involves the overall theory of level densities.

Shell and Pairing Effects in Level Densities. While, because of its difficulty, the problem of the strength functions associated with the collective features of the system has not yet received the amount of attention it deserves, other detailed features of the level densities have been worked out to a satisfactory degree. The level densities at low excitation energies are expected to be greatly influenced by the detailed structure of the single particle levels close to the Fermi surface, as well as by the two-body residual interaction. Recently a substantial success has been achieved in the development of a theoretical formalism which allows one to calculate the level density of a nucleus on the basis of a given shell model and of the pairing interaction.[19-30] The simplest Hamiltonian containing both features is the following:

$$H = \sum_{\pm k} \varepsilon_k \, a^{\dagger}_k \, a_k - G \sum a^{\dagger}_{k'} \, a^{\dagger}_{\bar{k}'} \, a_{\bar{k}} \, a_k \tag{16}$$

where ε_K are the shell model single particle energies, $a^{\dagger}_k$ and a_k are the creation and annihilation operators respectively, and G is the strength of the pairing interaction. The diagonal form of this Hamiltonian can be used to evaluate the Grand Partition function e^{Ω}:[27,28,30]

$$\Omega = \sum \beta(\varepsilon_k - \lambda - E_k) + 2 \sum \ln[1 + \exp - \beta(E_k - \gamma m_k)] + \sum \ln[1 + \exp - \beta(E_k + \gamma m_k)] - \frac{\beta\Delta^2}{G} \tag{17}$$

where m_k are the single particle spin projections, λ is the chemical potential, γ is the angular velocity, β is the reciprocal of the temperature, Δ is the gap parameter which indicates the extent of the pairing correlation, and $E_k = \sqrt{(\varepsilon_k - \lambda)^2 + \Delta^2}$ represent the energies of the intrinsic modes of excitation of the system (quasi-particles).

The boundary conditions are introduced in the formalism by means of the following equations:

$$\frac{\partial \Omega}{\partial \Delta} = 0 \text{ or } \sum \frac{1}{2E_k} [\tanh \tfrac{1}{2} \beta(E_k - \gamma m_k) + \tanh \tfrac{1}{2} \beta(E_k + \gamma m_k)] = \frac{2}{G} \quad \text{gap equation;} \tag{18}$$

$$\frac{\partial \Omega}{\partial \alpha} = N = \sum \left[1 - \frac{\varepsilon_k - \lambda}{2E_k} \left\{\tanh \tfrac{1}{2} \beta(E_k - \gamma m_k) + \tanh \tfrac{1}{2} \beta(E_k + \gamma m_k)\right\}\right] \quad \text{particle equation;} \tag{19}$$

$$\frac{\partial \Omega}{\partial \mu} = M = \sum m_k \left[\frac{1}{1 + \exp \beta(E_k - \gamma m_k)} - \frac{1}{1 + \exp \beta(E_k + \gamma m_k)}\right] \quad \text{angular momentum equation} \tag{20}$$

$$-\frac{\partial \Omega}{\partial \beta} = E = \sum \varepsilon_k \left[1 - \frac{\varepsilon_k - \lambda}{2E_k} \left\{\tanh \tfrac{1}{2} \beta(E_k - \gamma m_k) + \tanh \tfrac{1}{2} \beta(E_k + \gamma m_k)\right\}\right] - \frac{\Delta^2}{G}$$

energy equation (21)

where $\alpha = \beta\lambda$ and $\mu = \beta\gamma$. This set of four equations defines the quantities β, γ, λ, Δ in terms of E, M, N, G. This set of values is used to evaluate the entropy:

$$S = \Omega + \beta E - \alpha N - \mu M \tag{22}$$

The level density of the system is then obtained by means of the expression:

$$\rho = \frac{e^{S}}{(2M)^{n/2}\ D^{1/2}} \tag{23}$$

where n is the number of first integrals of motion which are explicitly considered in the problem, and

$$D = \det \left| \frac{\partial^2 \Omega}{\partial \alpha_i \partial \alpha_j} \right|$$

where α_i is the set of Lagrange multipliers associated with the first integrals of motion. Although very simple, the present formalism accounts rather well for the pairing effects, the shell effects, their mutual interaction and their dependence upon the excitation energy.

The pairing correlation, in the ground state, depends upon the single particle level density at the Fermi surface. When the nucleus is in a shell region, the single particle level density at the Fermi surface is small and the pairing effects are also small. The opposite occurs in an antishell region where the single particle level density is large and so is the pairing correlation. In other words, the pairing effects tend to counteract the shell effects: when the latter is large the former is small and vice versa.

As the excitation energy increases, the gap parameter Δ and the pairing correlation steadily decrease and eventually vanish because of the blocking effect of the quasi-particles. The shell effects also are washed away by the increasing excitation energy. This is due to the fact that the fluctuations in the single

particle level density are averaged out by the Fermi distribution. The statistical averaging function is in fact the negative derivative of the Fermi function, which becomes broader as the temperature and the excitation energy increase.

The angular momentum of the system is generated by breaking pairs and by aligning the spins of the resulting quasi-particle excitations. Each quasi-particle blocks a single particle level making it unavailable for the pairing interaction. Therefore, the pairing correlation and the gap parameter decrease and eventually vanish as the angular momentum increases. Some of the features discussed above can be observed in Fig. 3 and Fig. 4 where the results of a calculation based on the Nilsson model and on the pairing Hamiltonian are shown for the nucleus ^{220}Rn.[30] In Fig. 3 the dependence of the neutron gap parameter upon the temperature T and the angular momentum I is presented in the form of an isometric projection. The surface $\Delta(T,I)$ intersects the T,I plane along a curve which defines the boundary between the paired and the unpaired region. In Fig. 4 the level density surface is projected on the energy-angular momentum plane. The lower near-diagonal line in the figure represents the yrast line, or the locus of the states with lowest energy at fixed angular momentum. The boundaries between paired and unpaired phases for neutrons and protons are also shown. Their peculiar crossing is due to the way in which the angular momentum is shared between the neutron and proton components.

<u>Application of the Level Density Formalism to the Calculation of the Fission Probabilities</u>. In order to illustrate the effect of shells and pairing on the fission probabilities, the above formalism will be applied to superheavy nuclei.[35,36] For such nuclei the relevance of shell and pairing effects is overwhelming and a calculation applied to them does clearly display the features discussed above.

First the shell structure in the potential energy surface will be discussed. In Fig. 5c the potential energy of $^{296}_{116}X$ is shown as a function of the deformation parameter ε. This calculation has been performed using the Nilsson model and of the Strutinski normalization procedure. In the same figure the liquid drop potential energy is also shown as a function of ε. The latter curve shows that for this nucleus, whose fissionability parameter is close to unity, the liquid drop fission barrier is vanishingly small. The former curve shows that the shell structure generates a rather deep minimum at sphericity and, because of it, the nucleus is stabilized against fission by a barrier of about 7.5 MeV. Similar plots for other nuclei are shown in Fig. 5a-c.

In order to observe how the shell effects disappear with excitation energy, the level density at the ground state deformation and at the saddle point deformation can be calculated. This calculation is shown in Fig. 6. It can be observed that the saddle point level density rises faster than the ground state level density. In fact, the level density value reached at 60 MeV excitation energy by the nucleus in the ground state deformation is reached at about 7.5 MeV lower <u>local</u> excitation energy by the nucleus at the saddle point. Since the potential energy difference between the ground state and the saddle point is in fact 7.5 MeV, and since such a difference is exclusively due to the shell effects, it is possible to conclude that, at 60 MeV, the nucleus does not retain any relevant trace of shell effects. In order to better appreciate the evolution of the system as the excitation energy increases, it is possible to calculate, for each excitation energy, the probability of finding the nucleus at the various deformations. Assuming statistical coupling between the intrinsic modes and the collective fission mode, one obtains:[25,26]

$$P(E,\varepsilon)d\varepsilon = \frac{\sqrt{2\pi m}}{h} D^{-1/2} \rho(E_T)d\varepsilon \tag{24}$$

where E is the compound nucleus excitation energy, $E_T = E - V(\varepsilon)$ is the local excitation energy at the deformation ε,m is the inertia along the coordinate ε and $D = \left.\frac{d \ln \rho(x)}{dx}\right|_{x=E_T}$.

The natural logarithm of the deformation probability of $^{296}_{116}X$ is shown in Fig. 7b for various excitation energies. At low excitation energy, the deformation probability shows a marked peak at $\varepsilon = 0$ and a deep minimum at $\varepsilon = 0.225$. If the nucleus were stable against fission, the deformation probability would be bounded along any deformation coordinate. Since the system can undergo fission, the probability goes through a minimum and eventually diverges as the deformation increases. This minimum actually controls the flow of probability from the compound nucleus region to the region of forming fragments.[35,36] As the excitation energy increases, the structure of the deformation probability becomes less pronounced, the compound nucleus peak becomes broader and the rate-controlling minimum fills in. At the highest excitation energy, the deformation probability becomes almost flat from sphericity to the location of the fission barrier, indicating that the oscillations of the potential energy are completely irrelevant to the behavior of the excited system. In other words, the system behaves as if the fission barrier had vanished. Similar comments can be made about the nucleus $^{290}_{110}X$ whose deformation probability is shown in Fig. 7a. Another important point can be made in this discussion. The critical stage, or transition state, controlling the fission decay probability has been assumed, so far, to be located at the saddle point. The saddle point is an extremum in

the potential energy surface and does not have any direct connection with the phase space region which controls the decay. The deformation probability surface includes the overall phase space and determines the position of the transition state which is located on a saddle point which is unstable in n-1 degrees of freedom and stable along the fission mode. The locations of the deformation probability saddle point and of the potential energy saddle point in general do not coincide. In particular, the disappearence of the shell effects discussed above may be responsible for a shift in the location of the transition state.[35,36] Some evidence that this is occurring is available from the fission fragment angular distributions in the actinide region. The moment of inertia for the saddle point configuration appears in fact to shift from the expected value corresponding to the actual potential energy saddle point to the value consistent with the liquid drop saddle point.[21,29,50]

The final product of this formalism is the first chance fission probability shown for various isotopes in Figs. 8a-c. In order to obtain a reference point in the interpretation of these quantities one can use Eq. (7) as an approximation to the Γ_F/Γ_N expression. For a nucleus with $A \sim 300$, the temperature $T = 1$ MeV corresponds to an excitation energy between 30 and 40 MeV. When $B_F = B_N$ the fission probability at that temperature is $P_F \sim 0.1$. Similarly, in order to obtain $P_F = 0.5$, $B_N - B_F = 2.15$ MeV; for $P_F = 0.7$, $B_N - B_F = 2.88$ MeV; for $P_F = 0.8$, $B_N - B_F = 3.5$ MeV; for $P_F = 0.9$, $B_N - B_F = 6.35$ MeV. In all of these cases, the fission probability should decrease slowly with energy. An inspection of the fission probabilities calculated for the superheavy nuclei shows that for excitation energies larger than 35 MeV they assume very high values, as high as 0.95. Such high values are predicted by the Eq. (7) for neutron binding energies 4 to 6 MeV larger than the fission barriers. Since the

neutron binding energies are about 4 to 6 MeV, the effective barrier felt by these superheavy nuclei is practically zero. On the other hand, at lower excitation energies the effective barriers are very close to the true barriers. In particular, the fission probabilities are indeed very small for isotopes of element 114 and 116, where the shell effects are responsible for very large fission barriers. Furthermore, for nuclei where $B_F \sim B_N$ the fission probabilities are subjected to peculiar fluctuations at low energies mainly related to the different energy dependence of the pairing correlation at the saddle point and in the ground state (Fig. 8a).

Sec. IV. THE EXPERIMENTAL FISSION PROBABILITIES IN LIGHTER ELEMENTS

Extraction of the Total Fission Probabilities. The experimental data available for lighter elements at energies reasonably close to the barrier are proton and alpha induced fission cross sections as a function of energy for various targets ranging from the heavy rare earths to bismuth. The cross sections which are going to be analyzed here[16-18] are characterized by errors between 10% and 30%, due to various causes, such as uncertainties in the beam current reading, in the solid angle, in the detection efficiency, in the angular distributions and in the beam energy.

The observed fission events arise from two sources. The first and hopefully the main source is from the compound nucleus formed by the complete fusion of target and projectile with a subsequent thermalization of the kinetic energy. The second source is the compound nucleus formed after a direct reaction or a preequilibrium decay has taken place. The latter source is expected to be of minor importance in the first 20 MeV above the barrier, because of the strong energy dependence of the fission probability, but it is expected to be substantial in the high bombarding energy region. Even if one can disregard the contribution to fission due to direct reactions, one should estimate the fraction of the total reaction cross section associated with direct reactions. This is important in the calculation of the total fission probability: $P_{F,T} = \sigma_F/\sigma_C$, where σ_F and σ_C are the fission cross section and the compound nucleus cross section, respectively. Recent work in ^{4}He induced reactions in the Pb region[51] shows that the compound nucleus cross section is very close to the reaction cross section up to 55 MeV bombarding energy, it decreases by perhaps 30% with respect to the total cross section at 70 MeV, and may be a factor of 2 to 5 lower at 120 MeV. One of the greatest uncertainties is related to the precompound

emission of neutrons. For these reasons it is very hard to analyze the data above 70 MeV. The total fission probabilities up to this energy were determined by dividing the total fission cross section by the reaction cross section obtained by an optical model. The use of the optical model may produce systematic errors as large as 25%.

The First Chance Fission Probabilities. The quantity predicted by the theory is the first chance fission probability $P_{F,1} = \Gamma_F/(\Gamma_F + \Gamma_N)$. The experimental total fission probability $P_{F,T}$ includes also the probability that the nucleus undergoes fission after one or more neutrons have been emitted. The problem then arises of estimating the higher order fission probability in order to transform $P_{F,T}$ into $P_{F,1}$. In principle, if the total fission probability $P_{F,T}$ is available for two nuclei with the same Z and differing only by one neutron, it should be possible to extract $P_{F,1}$ for the heavier nucleus. Unfortunately, the various uncertainties associated with the experimental data, but especially the uncertainty in the compound nucleus cross section make this proceedure very dubious. The only safe conclusion which can be usually drawn is the establishment of an upper energy limit below which the contribution of higher order fission becomes unimportant.

One might also consider the possibility of obtaining a theoretical estimate of the higher order fission probability. Unfortunately, here the problem is even more serious. With a saddle temperature of about 2 MeV, a variation of 10% in the saddle single particle level density g_F produces a variation in $\frac{\Gamma_F}{\Gamma_N}$ of a factor of about 150! Even a small variation of 1% in g_F produces a variation of $\sim$ 70% in $\frac{\Gamma_F}{\Gamma_N}$! This means that any attempt to correct for higher order fission is likely to fail. Fortunately, the counterpart is more pleasant; large variations in the fission probabilities at high energies involve only minute changes in the single particle level density parameters. We shall make use of this conclusion later on.

In practice, the fission cross section is divided by the total reaction cross section and the resulting quantity is assumed to be equal to the total fission probability $P_{F,T}$ up to 25-30 MeV above the barrier where the contribution of higher order fission is small. In the next 10-15 MeV the effect of higher order fission is expected to be approximately counterbalanced by the decreasing compound nucleus cross section. Because of these reasons, it has been assumed that the above defined $P_{F,T}$ is also equal to $P_{F,1}$ or to $\frac{\Gamma_F}{\Gamma_T}$ up to 70 MeV excitation energy in ^{4}He induced fission.

Analysis of the Data. At this point one might be tempted to consider the possibility of comparing the experimental data directly with the theoretical fission probabilities calculated on the basis of the shell model. This attempt has been made by Vandenbosch and Mosel.[32] The results of such an investigation are shown in Fig. 9. The agreement between experiment and theory is rather poor as expected. The fission probabilities are very sensitive to the height of the fission barrier and to the ratio of the single particle level densities to be used in Γ_F and Γ_N. The present models do not reproduce both quantities accurately enough to justify any hope of immediate success for this approach.

An approach which leads to a better result is a hybrid formalism. In this formalism the neutron binding energy is taken from the experimental masses and the level density to be used in Γ_N is calculated from the Nilsson model and the pairing Hamiltonian. Insofar as the evaluation of Γ_F is concerned, the fission barrier height as well as the barrier penetrability are taken to be free parameters; the level density is evaluated on the basis of the uniform model and of the pairing Hamiltonian. The single particle level density at the saddle and the saddle gap parameter are also free parameters. The angular momentum is accounted for both in Γ_F and in Γ_N.

As it was discussed before, the use of the shell model in the evaluation of Γ_N does account for the ground state shell effects. One might then consider the possibility of accounting for the shell effects at the saddle point in the same way. This has been done by Britt et al.[33] in the analysis of the fission and isomer formation probabilities in the actinide region. In this work, however, it has been decided not to follow this approach for the following reasons. First, in the lead region and below, the shell effects in the neighborhood of the saddle

point are expected to be small because of the large deformation. Furthermore, the saddle point cannot be located in a shell region, because it would be a minimum, nor can it be in an antishell region because it would be a maximum. It must be somewhere between a shell and an antishell region which means, close to the liquid drop surface. This situation is quite different from that of the ground state which always is in a shell region, namely in a minimum. In other words the saddle masses are expected to be far smoother than the ground state masses. A superficial glance at some shell model calculations may give the impression that the shell fluctuations at the saddle are quite large. This impression is somewhat misleading and stems from an inadequate parameterization of the nuclear shape. In fact, a shell model calculation with a truncated deformation space has a tendency to locate the saddle point in an antishell region. When more collective degrees of freedom are introduced, the saddle moves toward the liquid drop surface in between a shell and an antishell region. Therefore, one may feel justified in using the uniform model for the evaluation of Γ_F because of the small shell effects to be expected at the saddle point, and furthermore because of a major lack of information about whatever shell structure does exist in the saddle region.

The formalism used in fitting the data contains five parameters which in principle can be considered to be free. In Γ_N one has the oscillator quantum $\hbar\omega_o$ which specifies the level spacing of the Nilsson model; in Γ_F, the barrier penetrability coefficient $\hbar\omega$; the fission barrier B_F; the density of the doubly degenerate single particle levels g_F; the gap parameter Δ assumed to be the same for neutrons and protons. Two different energy ranges have been studied. The first includes the data up to 70 MeV excitation energy and the second up to 120 MeV.

In a preliminary attempt to fit the data, all of the five parameters have been considered free. The most interesting result has been the large uncertainty with which both $\hbar\omega_o$ and g_F are determined. Equivalently good fits could be obtained by keeping the product of these two quantities constant and by adjusting the fission barrier in a minor way. This effect can be predicted on the basis of Eq. (7).

Because of the above conclusion, $\hbar\omega_o$ was assigned the value $41/A^{1/3}$ which contains the proper A dependence and should be reasonably accurate. The data were then fitted with the remaining four parameters. The resulting fits appear to be quite good and the parameters are essentially identical in both energy ranges. Some of the fits are shown in Fig. 10 and Fig. 11.

The barrier penetrabilities for those cases where data are available very close to the barrier have an average value of 1 MeV. The rather large dispersion observed in these quantities depends mainly upon the way in which the corrections for U or Th contaminants were performed close to the barrier.

In order to obtain a more consistent set of fission barriers, the barrier penetrability coefficients were fixed at 1 MeV. The fits obtained in this way are as good as the previous ones and the resulting parameters are shown in Table I. The fission barriers quoted in the table should be considered to be accurate within 1 MeV. Assuming that no shell effect are present at the saddle point, the experimental barriers from which the ground state shell effects are subtracted should follow closely the smooth liquid drop prediction. In Fig. 12 the experimental barriers corrected for the ground state shell effects and expressed in units of 1/600 of the surface energy of the corresponding spherical nucleus are plotted as a function of the fissionability parameter x. In the same graph the ground state shell effects are shown. The solid line represents the smooth liquid drop prediction. The experimental fluctuations about the liquid drop

value are at most 1 MeV, well within the experimental uncertainties. Therefore, one is led to the conclusion that the experimental shell effects at the saddle point are, for this region of elements, rather small.

The saddle single particle level densities are shown as a function of mass number in Fig. 13. The two lines bracketing the data correspond to the level density parameters $a_F = A/9$ and $a_F = A/8$ where $a_F = \frac{\pi^2}{3} g_F$. A reasonable average line passing through the data corresponds to $a_F = A/8.5$. The fluctuations about the average are smaller than 5%. When the fits are performed with Fermi gas level densities, the ratio a_F/a_N varies from about 1.0 in the upper rare earths to 1.5 in the ^{208}Pb shell region. Thus, it appears that the level densities based upon the Nilsson diagram have accounted for the major part of the shell effects and for their disappearence with energy. A closer examination shows that the deviations are not statistical in nature, but correlate quite well with the residual shell effects[52] not accounted for, or overaccounted for, by the Nilsson model. It is interesting to notice the average value of a_F, equal to A/8.5, as compared with the corresponding average quantity on Γ_N obtained by smoothing the shell model spectrum. This last quantity is $a_N = A/9.2$ giving a ratio $a_F/a_N = 1.08$. Although it is not possible at this stage to reach any definite conclusion regarding this experimental point, an increase in the saddle point single particle level density should be expected on the basis of a very simple argument. In a Fermi gas the single particle level density at the Fermi surface depends upon the particle density. The higher the particle density, the lower the single particle level density. The nuclear matter is less dense on the surface of the nucleus and the surface is larger in a deformed nucleus. Bishop et al.[53] have shown that the ratio of the single particle level densities at the Fermi surface for the

deformed to the undeformed nucleus is given by:

$$R = \frac{11}{15} + \frac{4}{45}\left(f^{-1} + 2f^{1/2}\right)$$

where $f^{3/2}$ is the ratio of the major to minor axis (Fig. 14). This ratio varies from 1.05 at x = .7 to 1.1 at x = 0.65 in surprising agreement with the experimental ratio of 1.08 obtained in the same fissionability range.

The saddle gap parameters Δ shown in Table I are characterized by rather large uncertainties. The only safe experimental indication is that the gap parameters are rather small. The average value is in fact somewhat smaller than the ground state value in the same region. While the large uncertainties associated with this quantity do not justify any serious speculation, it may be possible that the smallness of the gap parameters may be due to some extent to the rather large angular momentum with which the compound nuclei are prepared at excitation energies close to the barrier. The gap parameter and the pairing correlation are in fact diminished by the presence of angular momentum, as it can be seen in Fig. 3 and Fig. 4. It is also possible that this parameter is actually compensating for other quantities not included in the formalism, like the saddle point shell effects. In fact, pairing effects and shell effects behave much in the same way with excitation energy. However, if one assumes the decrease in pairing to be fully due to shell effects at the saddle point, such shell corrections would amount to 1 MeV at most.

Indications of a rather large gap parameter at the saddle point of ^{210}Po were obtained from the fission fragment angular distributions of the ^{4}He induced fission of ^{206}Pb and ^{207}Pb.[54] These very low energy angular distributions suggested a gap parameter as large as 1.5 MeV. The experiment

has been recently duplicated by Itkis et al.[55] with complete agreement on the data. While the high energy data seem to be consistent with $\Delta \sim 1$ MeV the lowest energy data remain unexplained with such a value. Shell model calculations are in progress to estimate the value of Δ necessary to fit the experimental data. While the fission probabilities are not the most sensitive quantities to use in the exploration of the superfluid properties of the system, the present analysis seems to indicate a saddle gap parameter definitely lower than 1.5 MeV.

CONCLUSION

It appears that the most relevant features associated with the fission probabilities are now understood in fair to good detail. The shell model, in conjunction with the liquid drop model can provide a nearly quantitative description of the potential energies relevant to the problem. At the same time the statistical-thermodynamical behavior of the system can be predicted in an equivalently good detail. In fact, a new picture is emerging where the ground state and the saddle point properties are discussed on the same basis as the statistical properties of the compound nucleus and of the transition state. The same physical structure responsible for the anomolously small masses of nuclei in the ^{208}Pb region is seen to be responsible for the unusually high fission barriers of the same nuclei and for the very rapid increase in their fission probabilities.

It is to be recognized that the present status of the theory still falls short of a completely quantitative understanding. The fission barriers cannot be predicted with accuracies better than a few MeV and similar difficulties are

encountered in reliably predicting the details of the potential energies. The same uncertainties in the shell structure affect the evaluation of the level densities and of other related statistical quantities. Furthermore, in the actinide region where the fission probabilities can be observed at extremely low energies above the barrier, delicate problems arise associated with the inapplicability of statistical mechanics and to the onset of fluctuations requiring more of a spectroscopical than a statistical interpretation.

ACKNOWLEDGMENTS

It is a pleasure to thank Dr. S. G. Thompson for his valuable comments on the paper; Mr. R. C. Gatti, and Mrs. D. Valentine are thanked for their help with some of the figures.

FOOTNOTES AND REFERENCES

*Work performed under the auspices of the U. S. Atomic Energy Commission.

1. N. Bohr and J. A. Wheeler, Phys. Rev. 56, 426 (1939).
2. L. Meitner and O. R. Frish, Nature 143, 239 (1939).
3. V. F. Weisskopf, Phys. Rev. 52, 295 (1937).
4. J. A. Wheeler, Channel Analysis of Fission, Fast Neutron Physics, ed. by J. B. Marion and J. L. Fowler (Interscience Publishers, New York - London, 1963), Part II, 2051.
5. R. Vandenbosch and J. R. Huizenga, Proceeding of the Second United Nations International Conference on the Peaceful Uses of Atomic Energy, 15, P/688 (United Nations, Geneva, 1958) 286.
6. H. R. Huizenga and R. Vandenbosch, Nuclear Fission, in Nuclear Reactions, ed. by P. M. Endt and P. B. Smith (North-Holland Publishing Co., Amsterdam, 1962), Vol. II.
7. G. N. Flerov, Proceedings of the Second United Nations International Conference on the Peaceful Uses of Atomic Energy, 14, P/2299 (United Nations, Geneva, 1958) 151.
8. Baraboshkin, Karamyam, and Flerov, J. Exptl. Theoret. Phys. (USSR), 32, 1294 (1957).
9. Karamyan, Gerlit, and Myasoedov, J. Exptl. Theoret. Phys. (USSR), 36, 621 (1959).
10. Druin, Polikanov, and Flerov, J. Exptl. Theoret. Phys. (USSR), 32, 1298 (1957).
11. S. M. Polikanov and V. A. Druin, J. Exptl. Theoret. Phys. (USSR), 36, 744 (1959).
12. V. A. Karnankhov, J. Exptl. Theoret. Phys. (USSR), 36, 1933 (1959).
13. J. R. Huizenga, R. Chaudhry, and R. Vandenbosch, Phys. Rev. 126, 210 (1962).
14. D. S. Burnett, R. C. Gatti, F. Plasil, B. P. Price, W. J. Swiatecki, and S. G. Thompson, Phys. Rev. 134, 952 (1964).

15. T. Sikkeland, Phys. Rev. 135, 669 (1964).

16. A. Kodai-Joopari, Ph.D. Thesis, University of California, Lawrence Radiation Laboratory Report UCRL-16489 (1966).

17. G. M. Raispeck and J. W. Cobble, Phys. Rev. 153, 1270 (1967).

18. L. G. Moretto, R. C. Gatti, and S. G. Thompson, Lawrence Radiation Laboratory Report UCRL-17989, Nuclear Chemistry Division Annual Report, January 1968, p. 141.

19. F. C. Williams, Nucl. Phys. A133, 33 (1968).

20. L. G. Moretto, R. Stella, and V. Caremella-Crespi, Energia Nucleare 17, 436 (1970).

21. V. S. Ramamurthy, S. S. Kapoor, and S. K. Kataria, Phys. Rev. Letters 25, 386 (1970).

22. F. C. Williams, G. Chan, and J. R. Huizenga, Nucl. Phys. A187, 225 (1972).

23. M. Hillman and J. R. Grover, Phys. Rev. 185, 1303 (1969).

24. P. Decowski, W. Grochulski, A. Marcinkowski, K. Siwek, and Z. Wilhelmi, Nucl. Phys. A110, 129 (1968).

25. L. G. Moretto and R. Stella, Phys. Letters 32B, 558 (1970).

26. L. G. Moretto, Nucl. Phys. A182, 641 (1972).

27. L. G. Moretto, Phys. Letters 35B, 379 (1971).

28. L. G. Moretto, Nucl. Phys. A185, 145 (1972).

29. M. Sano and M. Wakai, Prog. Theor. Phys. 48, 160 (1972).

30. L. G. Moretto, Lawrence Berkeley Laboratory Report LBL-1298 (1972).

31. L. G. Moretto, S. G. Thompson, J. Routti, and R. C. Gatti, Phys. Letters 38B, 471 (1972).

32. R. Vandenbosch and V. Mosel, Phys. Rev. Letters 28, 1726 (1972).

33. H. C. Britt, M. Bolsterli, J. R. Nix, and J. L. Norton, Los Alamos Laboratory Report LA-DC-72-1307, November 1972.

34. V. Metag, S. M. Lee, E. Liukkonen, G. Sletten, S. Bjørnholm, and A. S. Jensen, preprint.

35. L. G. Moretto, Phys. Letters 34B, 191 (1971).

36. L. G. Moretto, Nucl. Phys. A180, 337 (1972).

37. V. S. Ramamurthy and S. S. Kapoor, Proceeding of the Nuclear Physics and Solid State Physics Symposium, Madurai-India (1972), Vol. 2, p. 279.

38. D. L. Hill and J. A. Wheeler, Phys. Rev. 89, 1102 (1953).

39. T. Ericson, Advan. Phys. 9, 425 (1960).

40. S. Cohen, F. Plasil, and W. J. Swiatecki, Proceedings of the Third Conference on Reactions Between Complex Nuclei, ed. by A. Ghiorso, R. M. Diamond, and H. A. Conzett, University of California Press (1963), p. 325.

41. S. Cohen and W. J. Swiatecki, Ann. Phys. (New York) 19, 67 (1962); ibid. 22, 406 (1963).

42. S. Cohen, F. Plasil, and W. J. Swiatecki, Lawrence Berkeley Laboratory Report LBL-1502 (1972).

43. For a recent review on Nuclear Level Densities, see: J. R. Huizenga and L. G. Moretto, Ann. Rev. Nucl. Sci. 22, 427 (1972).

44. H. Bethe, Phys. Rev. 50, 332 (1936).

45. D. W. Lang, Nucl. Phys. 77, 545 (1965).

46. H. Baba, Nucl. Phys. A159, 625 (1970).

47. U. L. Businaro and S. Gallone, Nuovo Cimento 1, 629 (1955).

48. J. R. Nix, Ph.D. Thesis, University of California, Lawrence Radiation Laboratory Report UCRL-11338 (1964).

49. L. D. Landau and E. M. Lifshitz, Statistical Physics (Addison-Wesley Publishing Company, Inc., Reading, Mass., 1958), p. 86.

50. R. Vandenbosch, preprint.

51. R. Bimbot et Y. Le Beyec, J. Physique 32, 243 (1971).

52. S. G. Nilsson, C. F. Tsang, A. Sobiczewski, Z. Szymanski, S. Wychech, G. Gustafson, J. L. Lamm, P. Moeller, and B. Nilsson, Nucl. Phys. A131, 1 (1969).

53. C. J. Bishop, I. Halpern, R. W. Shaw, Jr., and R. Vandenbosch, Nucl. Phys. A198, 161 (1972).

54. L. G. Moretto, R. C. Gatti, S. G. Thompson, J. R. Huizenga, and J. O. Rasmussen, Phys. Rev. 178, 1845 (1969).

55. M. G. Itkis, K. G. Kuvatov, V. N. Okolovich, G. Ya. Ruskina, G. N. Smirenkin, and A. S. Tishin, Yad. Fiz. 16, 958 (1972); Translation Sov. J. Nucl. Phys. 16, 144 (1973).

Table 1. Parameters obtained from the analysis of fission probabilities.[31]

Reaction	Ref.	B_f (MeV)	g_f (MeV^{-1})	Δ (MeV)
$^{209}_{83}Bi + ^{4}_{2}He \rightarrow ^{213}_{85}At$	[16]	17.0	7.67	0.38
$^{208}_{82}Pb + ^{4}_{2}He \rightarrow ^{212}_{84}Po$	[16]	19.5	7.36	0.06
$^{207}_{82}Pb + ^{4}_{2}He \rightarrow ^{211}_{84}Po$	[16]	19.7	7.08	0.84
$^{206}_{82}Pb + ^{4}_{2}He \rightarrow ^{210}_{84}Po$	[16]	20.5	7.42	0.60
$^{209}_{83}Bi + ^{1}_{1}H \rightarrow ^{210}_{84}Po$	[16]	21.4	7.33	0.17
$^{208}_{82}Pb + ^{1}_{1}H \rightarrow ^{209}_{83}Bi$	[16]	23.3	7.55	0.22
$^{206}_{82}Pb + ^{1}_{1}H \rightarrow ^{207}_{83}Bi$	[16]	21.9	7.63	0.11
$^{197}_{79}Au + ^{4}_{2}He \rightarrow ^{201}_{81}Tl$	[16]	22.3	7.57	0.39
$^{197}_{79}Au + ^{1}_{1}H \rightarrow ^{198}_{80}Hg$	[16]	20.4	7.43	0.68
$^{187}_{75}Re + ^{4}_{2}He \rightarrow ^{191}_{77}Ir$	[17]	23.7	7.16	0.05
$^{185}_{75}Re + ^{4}_{2}He \rightarrow ^{189}_{77}Ir$	[17]	22.6	6.84	0.10
$^{184}_{74}W + ^{4}_{2}He \rightarrow ^{188}_{76}Os$	[18]	24.2	6.89	0.54
$^{183}_{74}W + ^{4}_{2}He \rightarrow ^{187}_{76}Os$	[18]	22.7	6.84	0.83
$^{182}_{74}W + ^{4}_{2}He \rightarrow ^{186}_{76}Os$	[18]	23.4	6.66	0.43
$^{181}_{83}Ta + ^{4}_{2}He \rightarrow ^{185}_{75}Re$	[16]	24.0	6.51	0.60
$^{175}_{71}Lu + ^{4}_{2}He \rightarrow ^{179}_{73}Ta$	[17]	26.1	6.53	0.99
$^{169}_{69}Tm + ^{4}_{2}He \rightarrow ^{173}_{71}Lu$	[17]	28.0	6.17	0.87

The barrier penetrations have been set equal to 1.0 MeV.

FIGURE CAPTIONS

Fig. 1. Examples of ^{4}He induced fission cross sections in lighter elements. The data are taken from Ref. 13, 14, 16-18.

Fig. 2. Examples of ^{1}H induced fission cross sections on lighter elements. The data are taken from Ref. 16.

Fig. 3. Isometric projection of the neutron gap parameter as a function of temperature and angular momentum for the neutron component of $^{220}_{86}$Rn.[30] The angular momentum refers to the neutron component only.

Fig. 4. Lines of constant natural logarithm of the level density in the energy-angular momentum plane for the nucleus $^{220}_{86}$Rn.[30] The lowest line going diagonally from lower left to upper right is the yrast line. The boundaries of the neutron and proton superfluid phases are also shown.

Fig. 5. Potential energy profiles[36] of some superheavy nuclei calculated on the basis of the liquid drop model (solid line) and of the Strutinski method (solid line with dots)

Fig. 6. Level densities as a function of local excitation energy[36] calculated for the ground state and saddle point deformation of $^{296}_{116}$X.

Fig. 7. Logarithms of the deformation probabilities at various excitation energies[36] for the nuclei $^{290}_{110}$X (a) and $^{296}_{110}$X (b).

Fig. 8. First chance fission probabilities for various superheavy nuclei.[36]

Fig. 9. Comparison between some experimental fission probabilities and some shell model calculations.[32]

Fig. 10. Least-squares fits to the fission probabilities of some compound nuclei produced with proton bombardment.[31]

Fig. 11. Least-squares fits to the fission probabilities of some compound nuclei produced with ^{4}He bombardment.[31]

Fig. 12. Experimental fission barriers corrected for the ground state shell effects (upper points) and ground state shell effects (lower points) as a function of the fissionability parameter. The solid line represents the smooth liquid drop prediction.[31]

Fig. 13. Experimental saddle point single particle level densities as a function of mass number. The two dashed lines correspond to a level density parameter a equal to A/8 and A/9, respectively.[13]

Fig. 14. Ratio of the single particle level densities for a deformed and a non-deformed Fermi gas nucleus as a function of the major to minor axis ratio.[53]

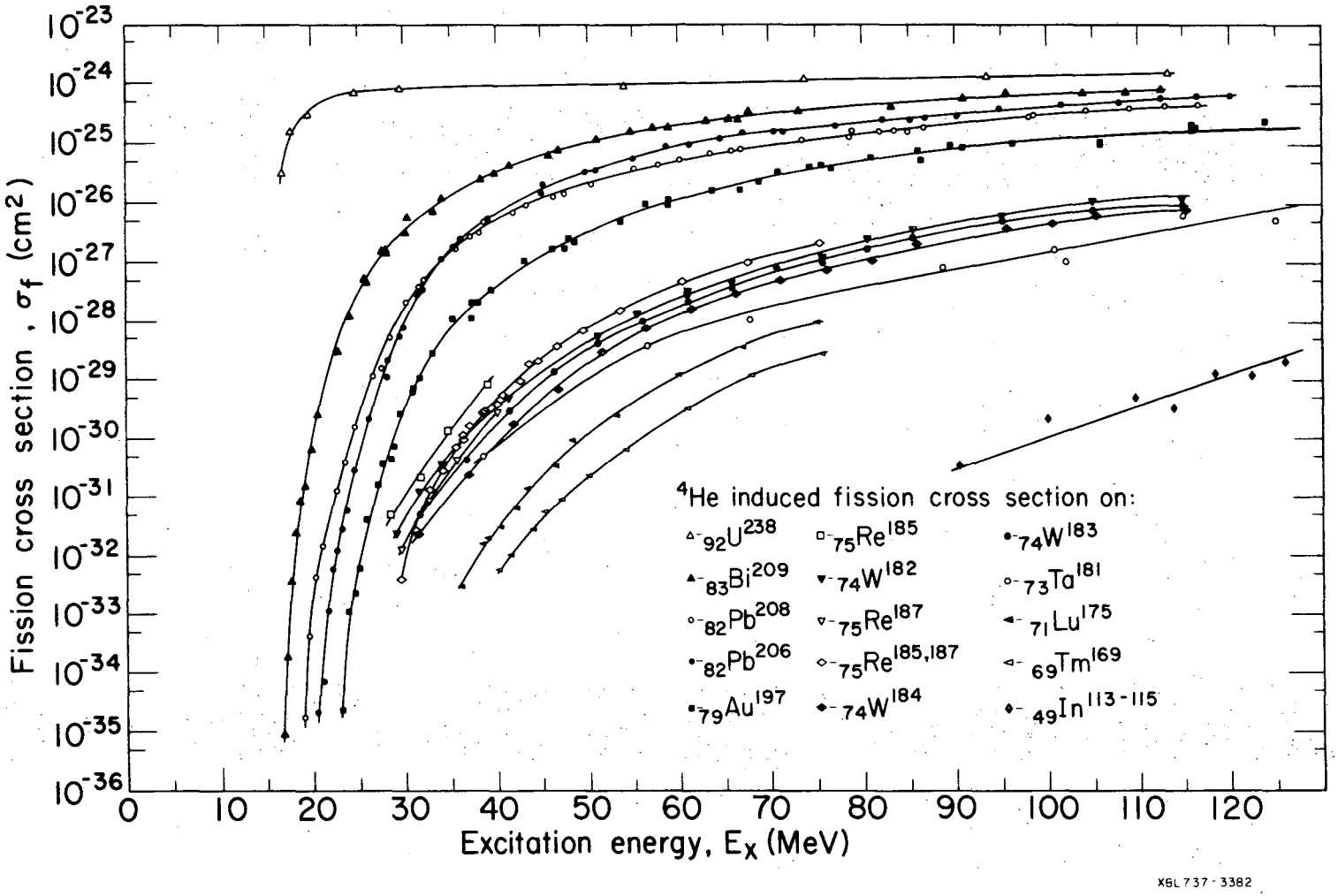
Fission cross section, σ_f (cm^2)
10^{-23}
10^{-24}
10^{-25}
10^{-26}
10^{-27}
10^{-28}
10^{-29}
10^{-30}
10^{-31}
10^{-32}
10^{-33}
10^{-34}
10^{-35}
10^{-36}
0 10 20 30 40 50 60 70 80 90 100 110 120
Excitation energy, E_x (MeV)
^{4}He induced fission cross section on:
$_{92}U^{238}$
$_{83}Bi^{209}$
$_{82}Pb^{208}$
$_{82}Pb^{206}$
$_{79}Au^{197}$
$_{75}Re^{185}$
$_{74}W^{182}$
$_{75}Re^{187}$
$_{75}Re^{185,187}$
$_{74}W^{184}$
$_{74}W^{183}$
$_{73}Ta^{181}$
$_{71}Lu^{175}$
$_{69}Tm^{169}$
$_{49}In^{113-115}$
XBL 737-3382

Fig. 1

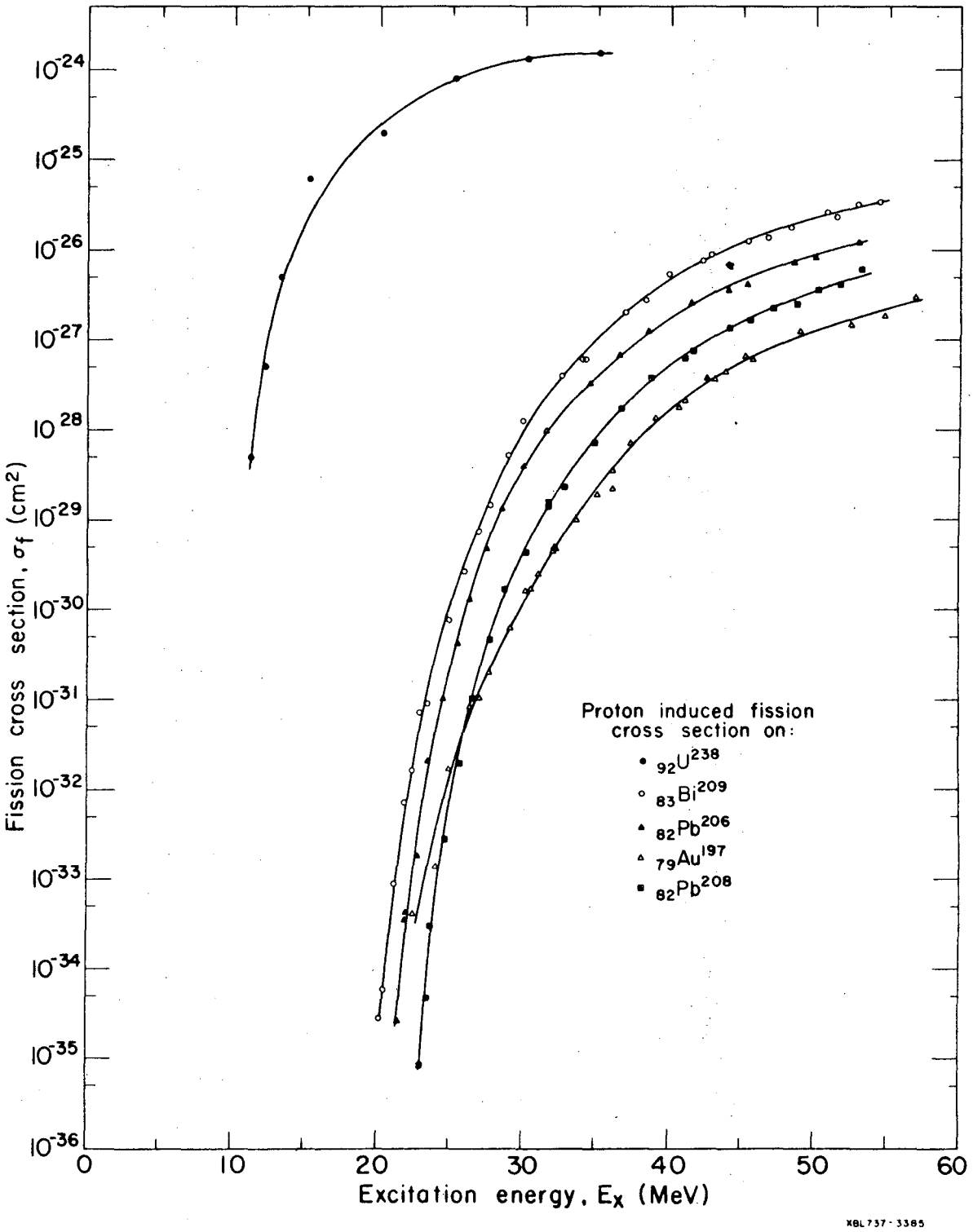
Fission cross section, σ_f (cm^2)
10^{-24}
10^{-25}
10^{-26}
10^{-27}
10^{-28}
10^{-29}
10^{-30}
10^{-31}
10^{-32}
10^{-33}
10^{-34}
10^{-35}
10^{-36}
0
10
20
30
40
50
60
Excitation energy, E_x (MeV)
Proton induced fission cross section on:
$_{92}U^{238}$
$_{83}Bi^{209}$
$_{82}Pb^{206}$
$_{79}Au^{197}$
$_{82}Pb^{208}$
XBL 737-3385

Fig. 2

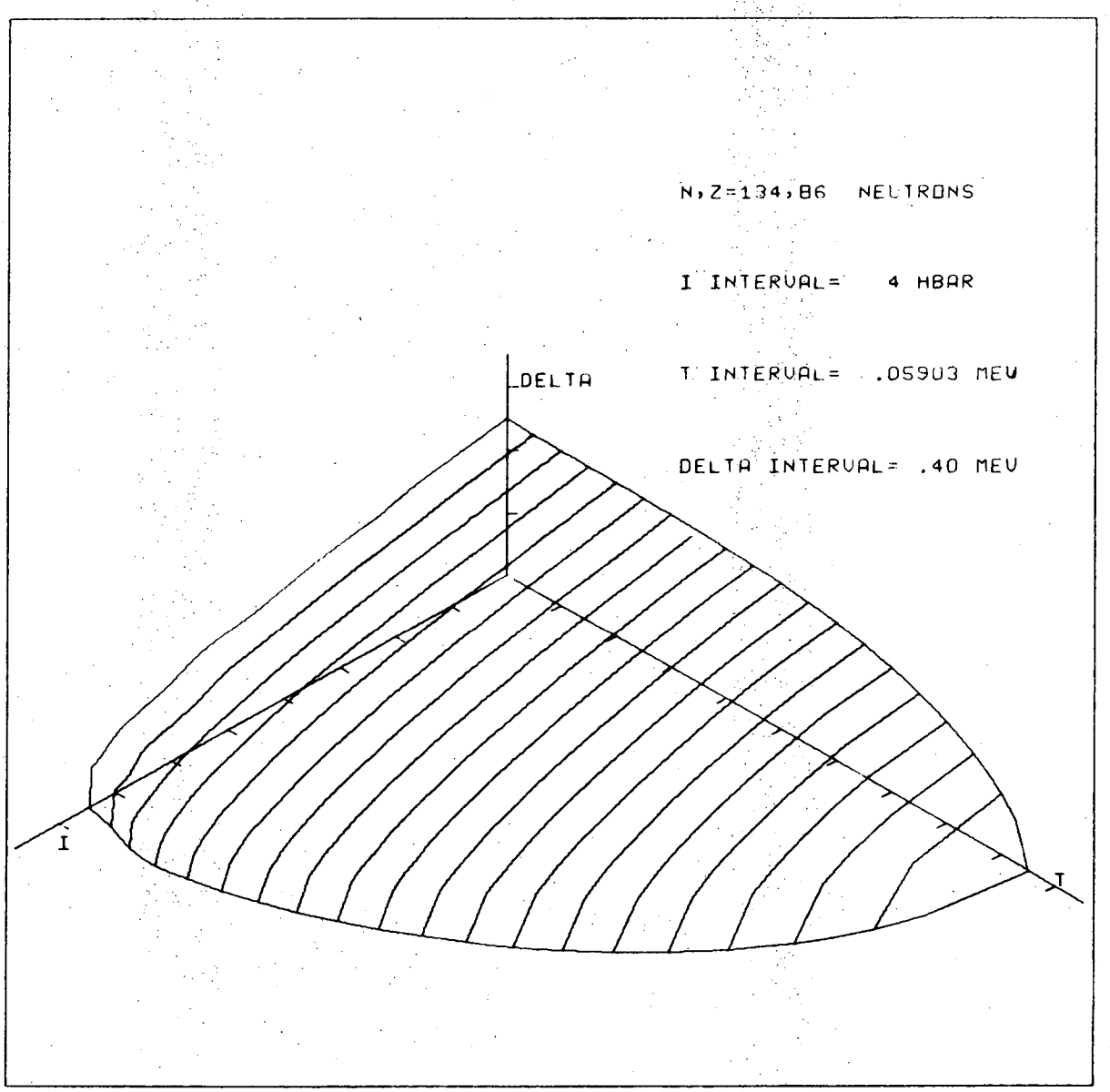

XBL 733-273

Fig. 3

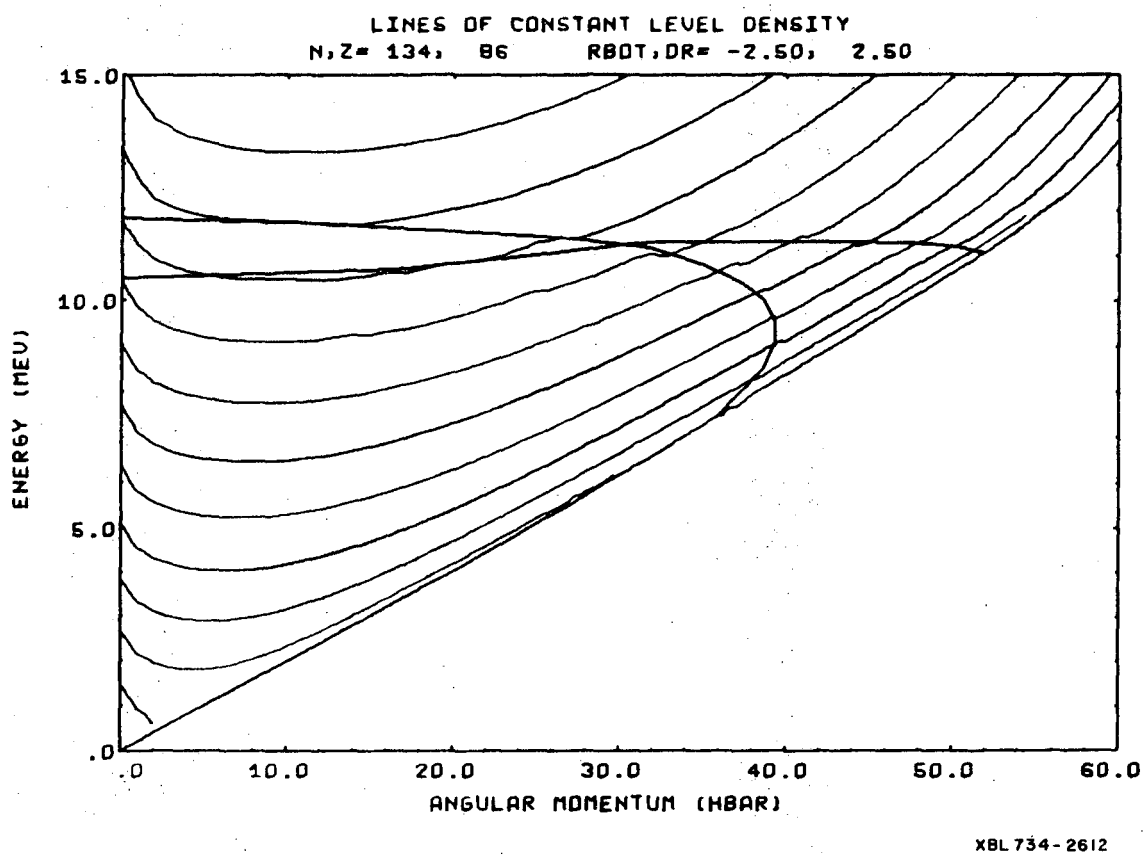
LINES OF CONSTANT LEVEL DENSITY
N,Z= 134, 86 RBOT,DR= -2.50, 2.50
15.0
10.0
5.0
.0
ENERGY (MEV)
.0
10.0
20.0
30.0
40.0
50.0
60.0
ANGULAR MOMENTUM (HBAR)
XBL 734-2612

Fig. 4

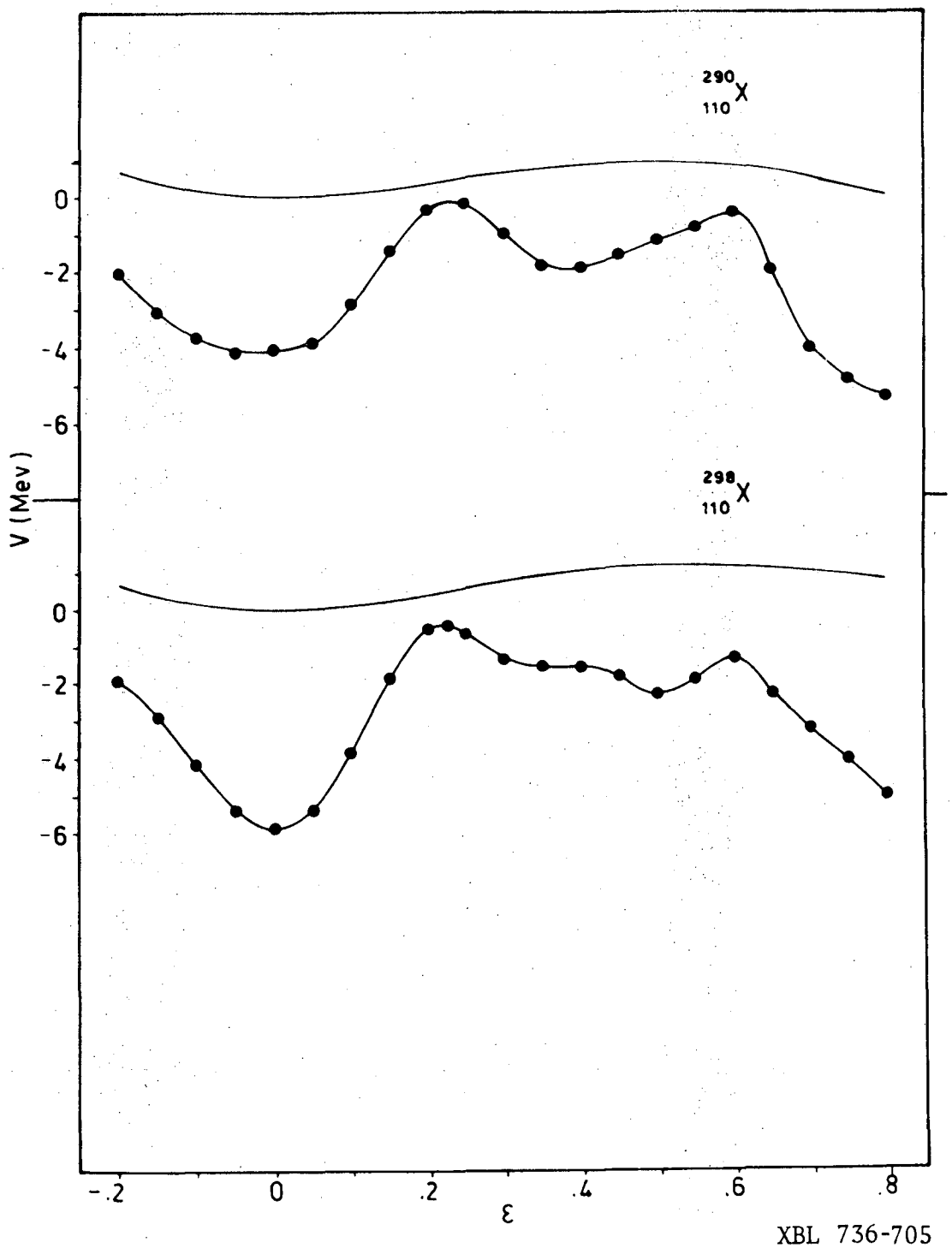

Fig. 5a

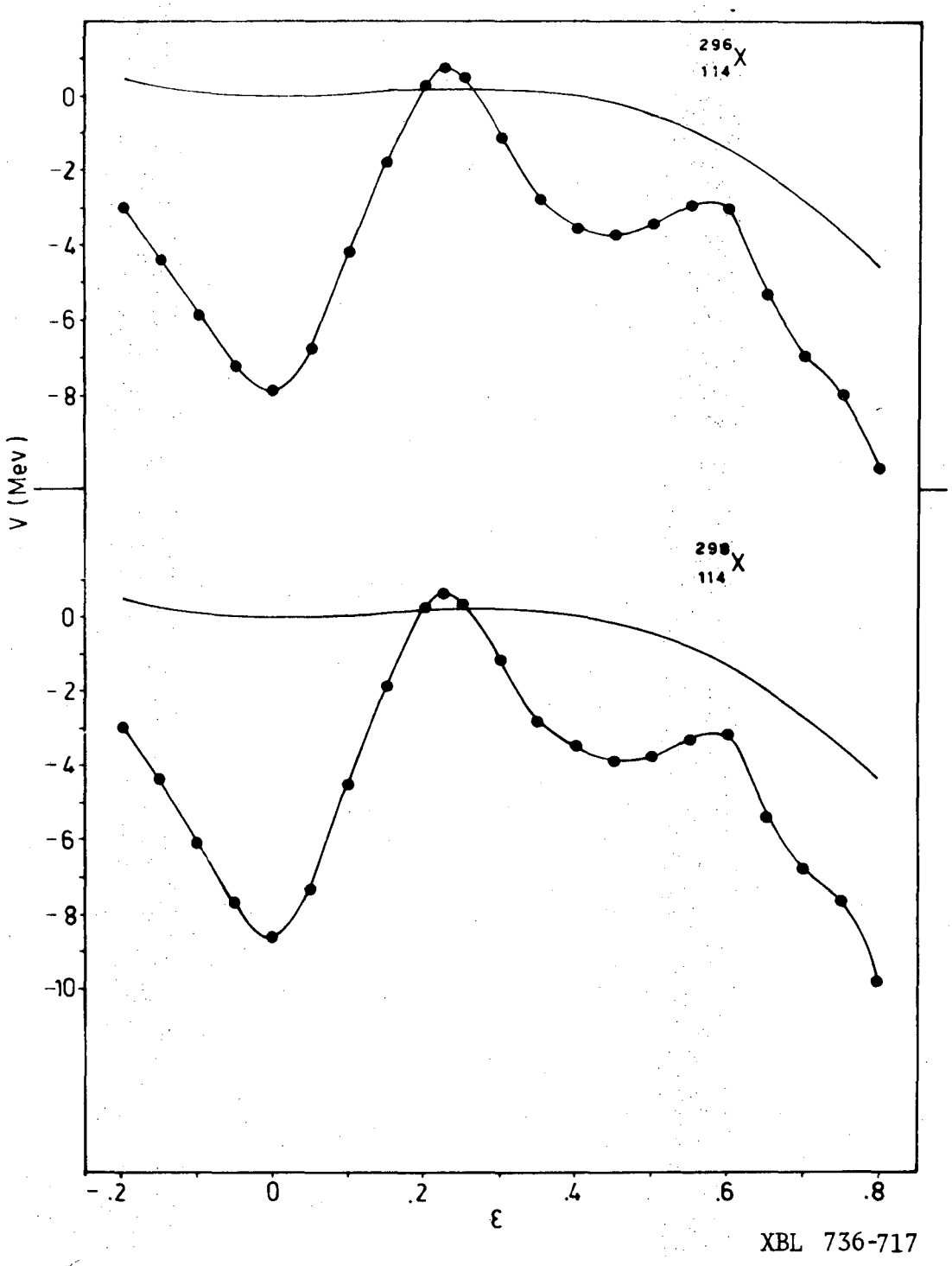

Fig. 5b

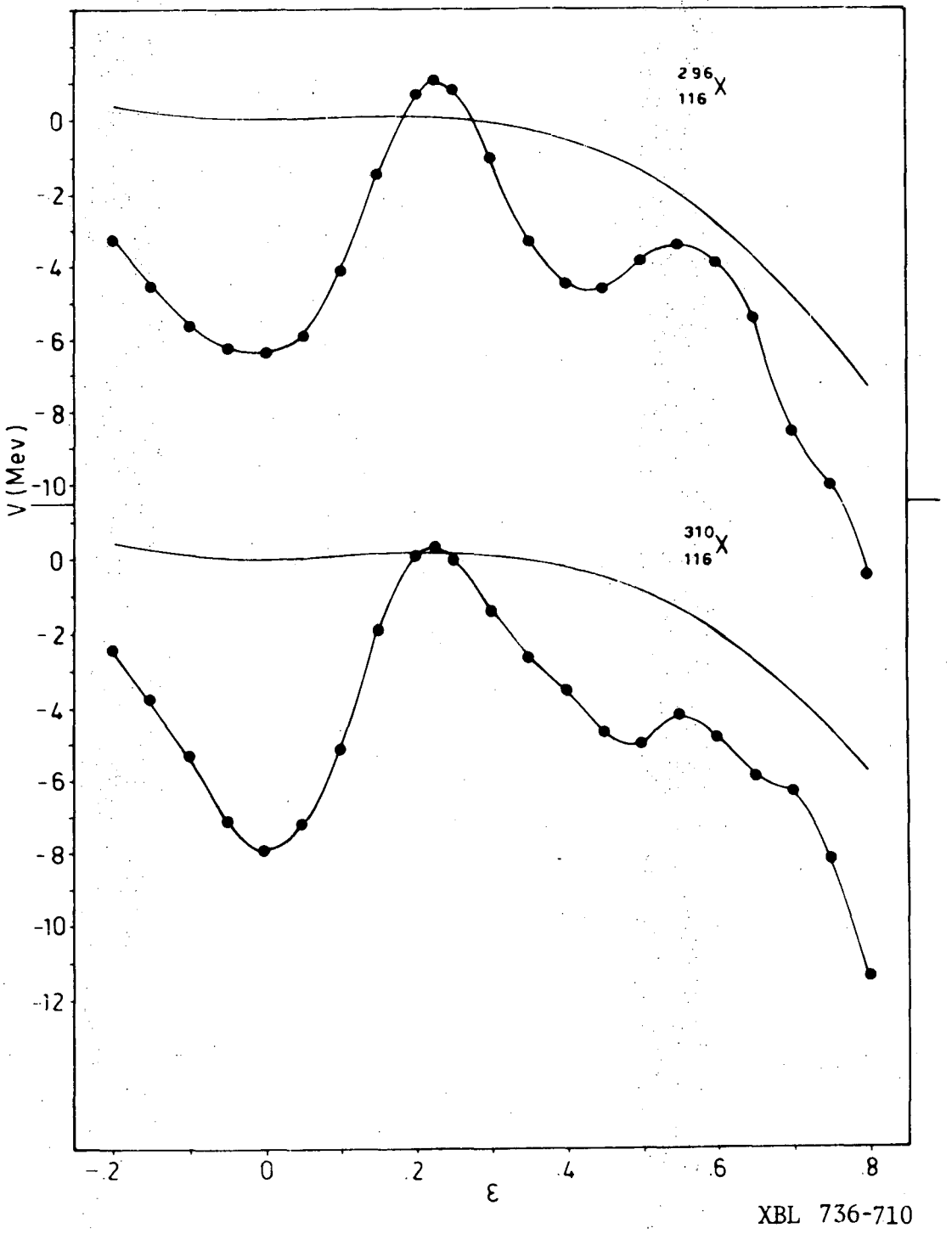

Fig. 5c

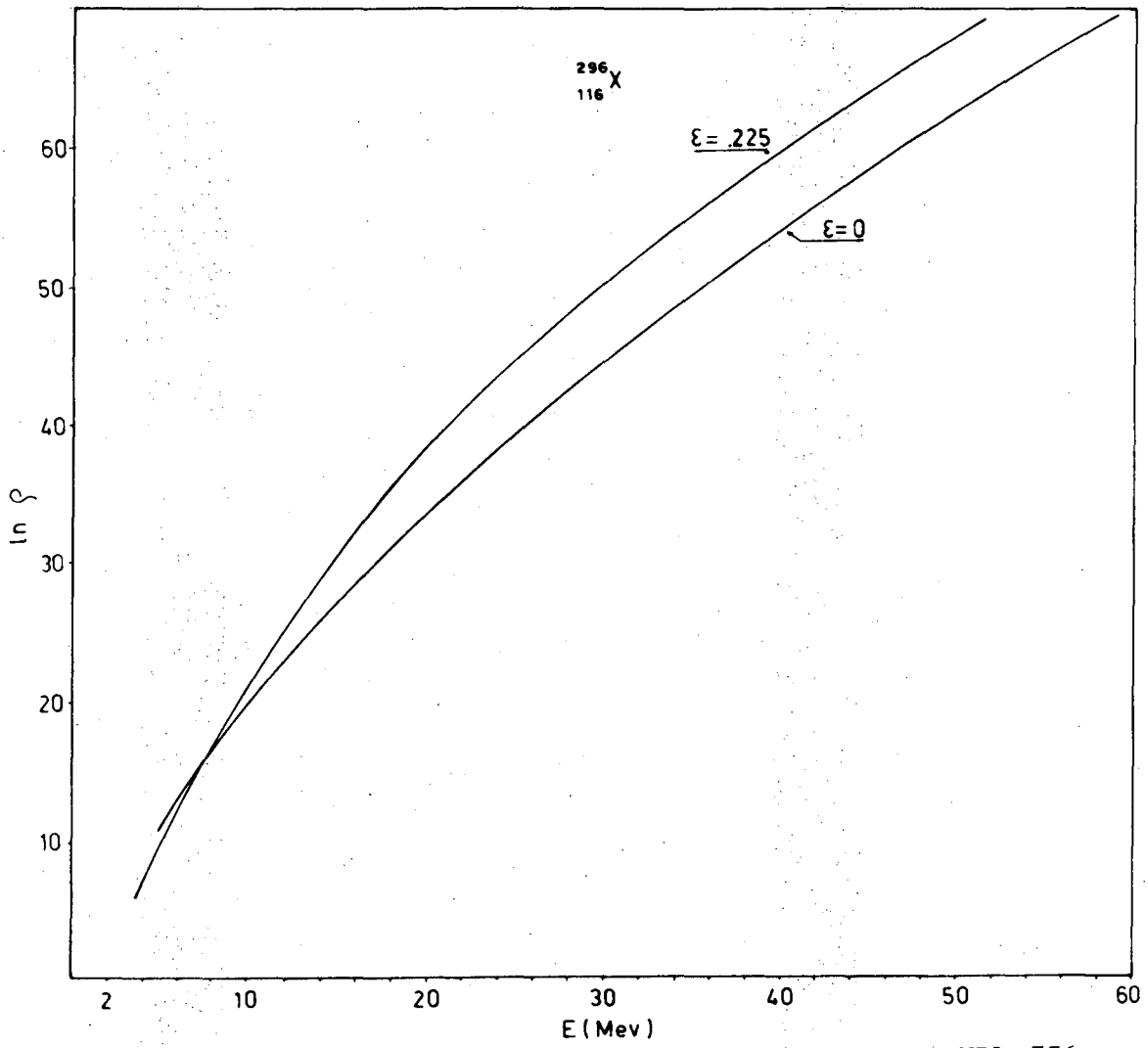

XBL 736-715

Fig. 6

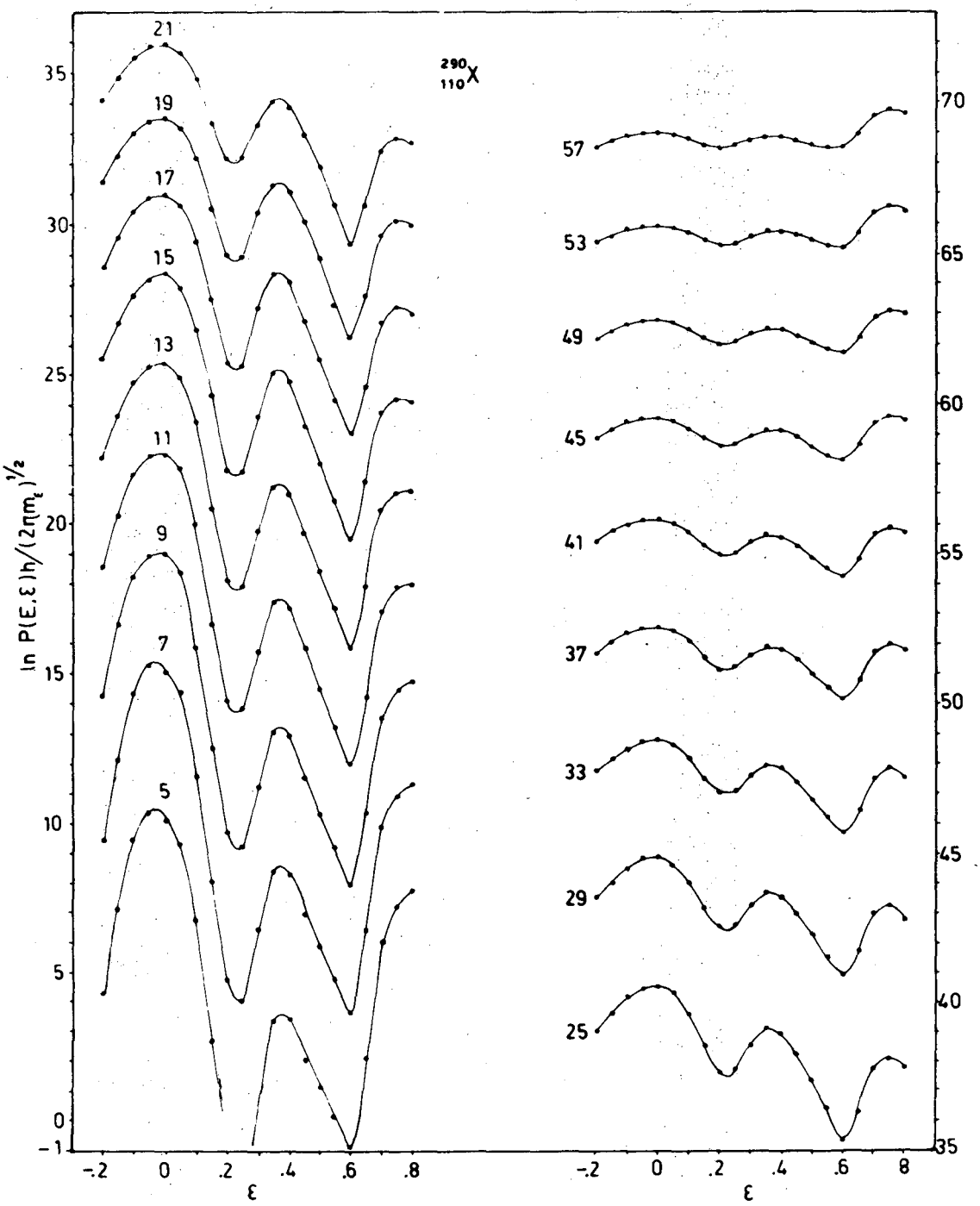

XBL 736-708

Fig. 7a

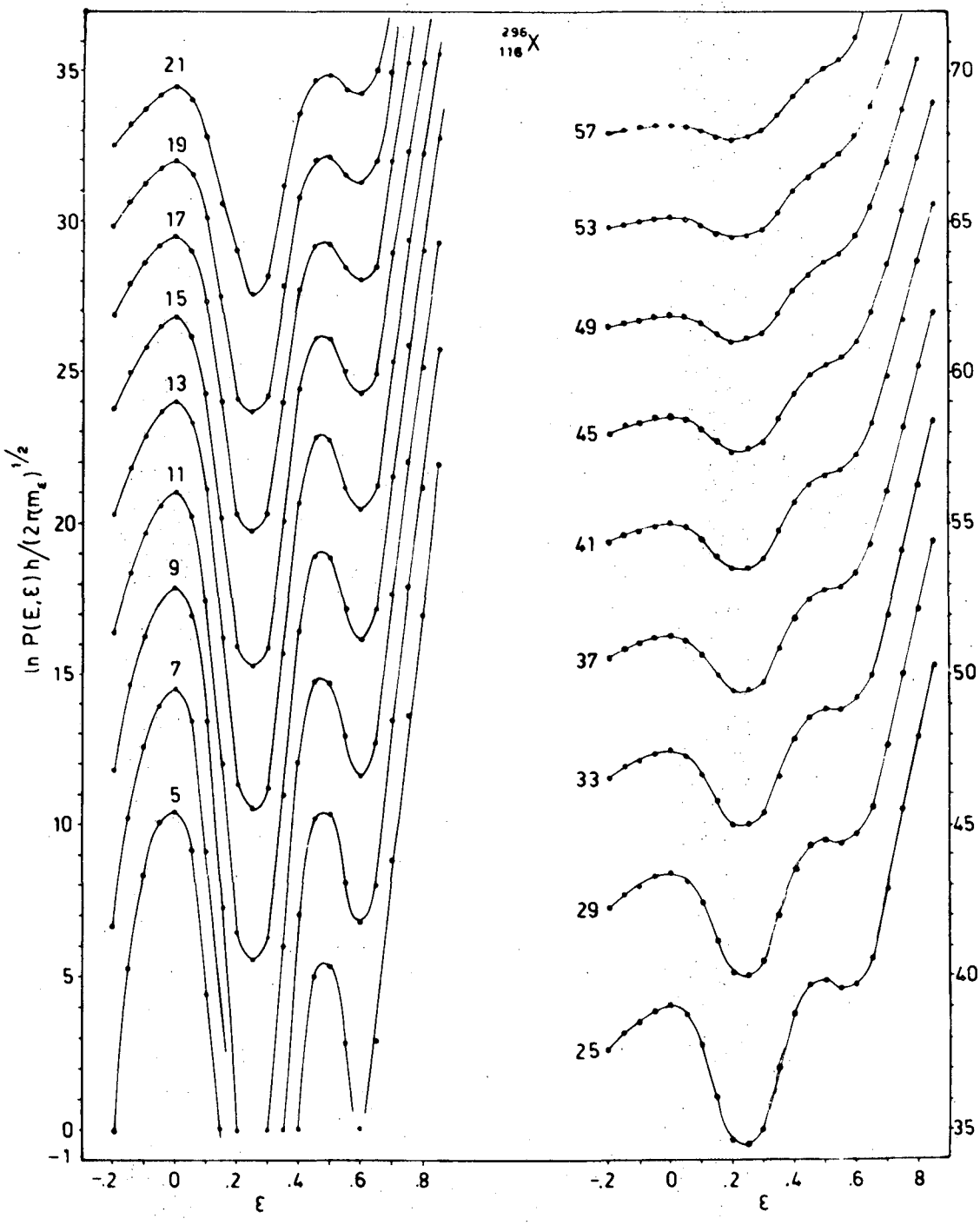

XBL 736-707

Fig. 7b

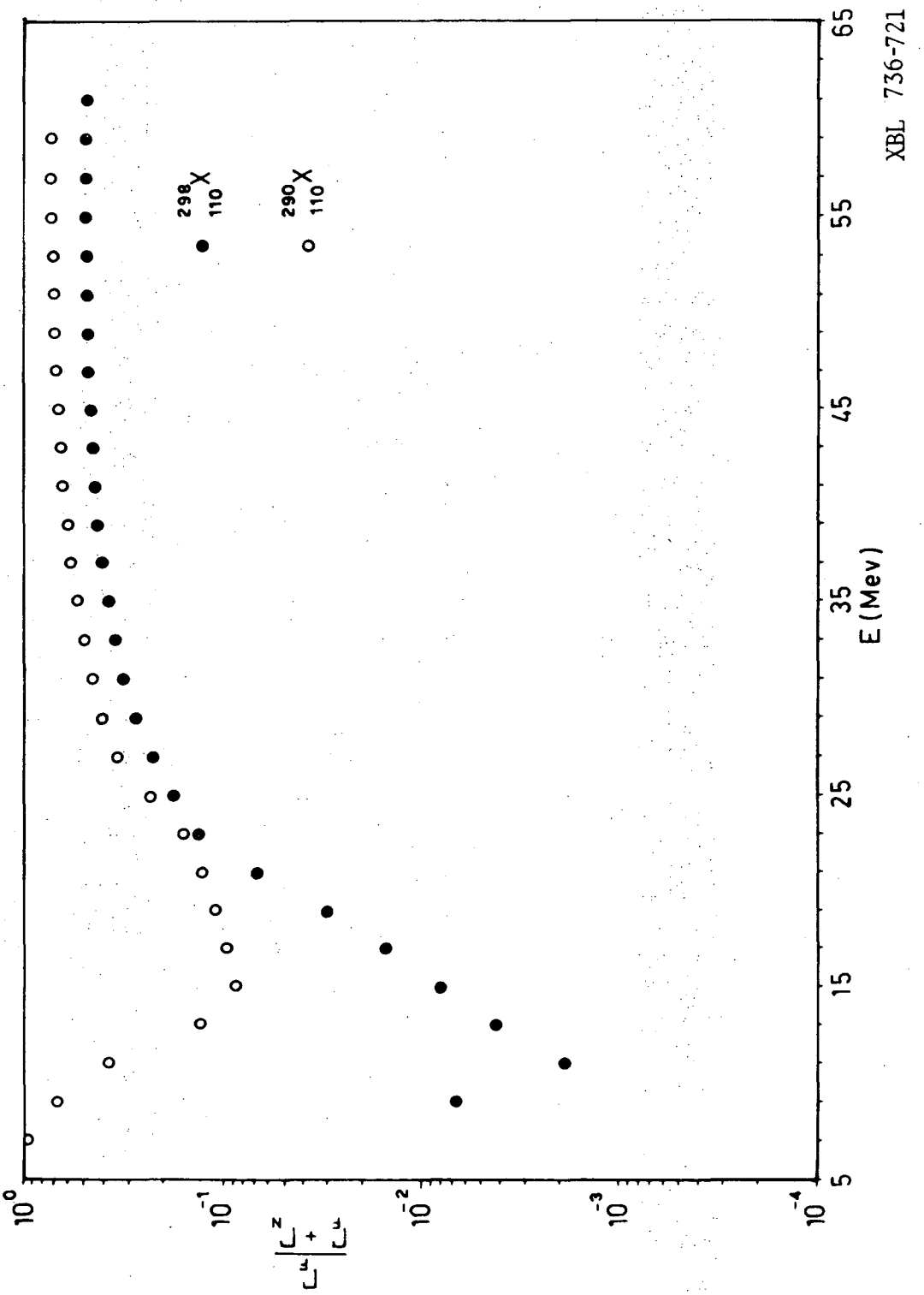
298
110
X
290
110
X
E (Mev)
5
15
25
35
45
55
65
10^0
10^{-1}
10^{-2}
10^{-3}
10^{-4}
$\frac{\sigma^N + \sigma^J}{\sigma^J}$
XBL 736-721

Fig. 8a

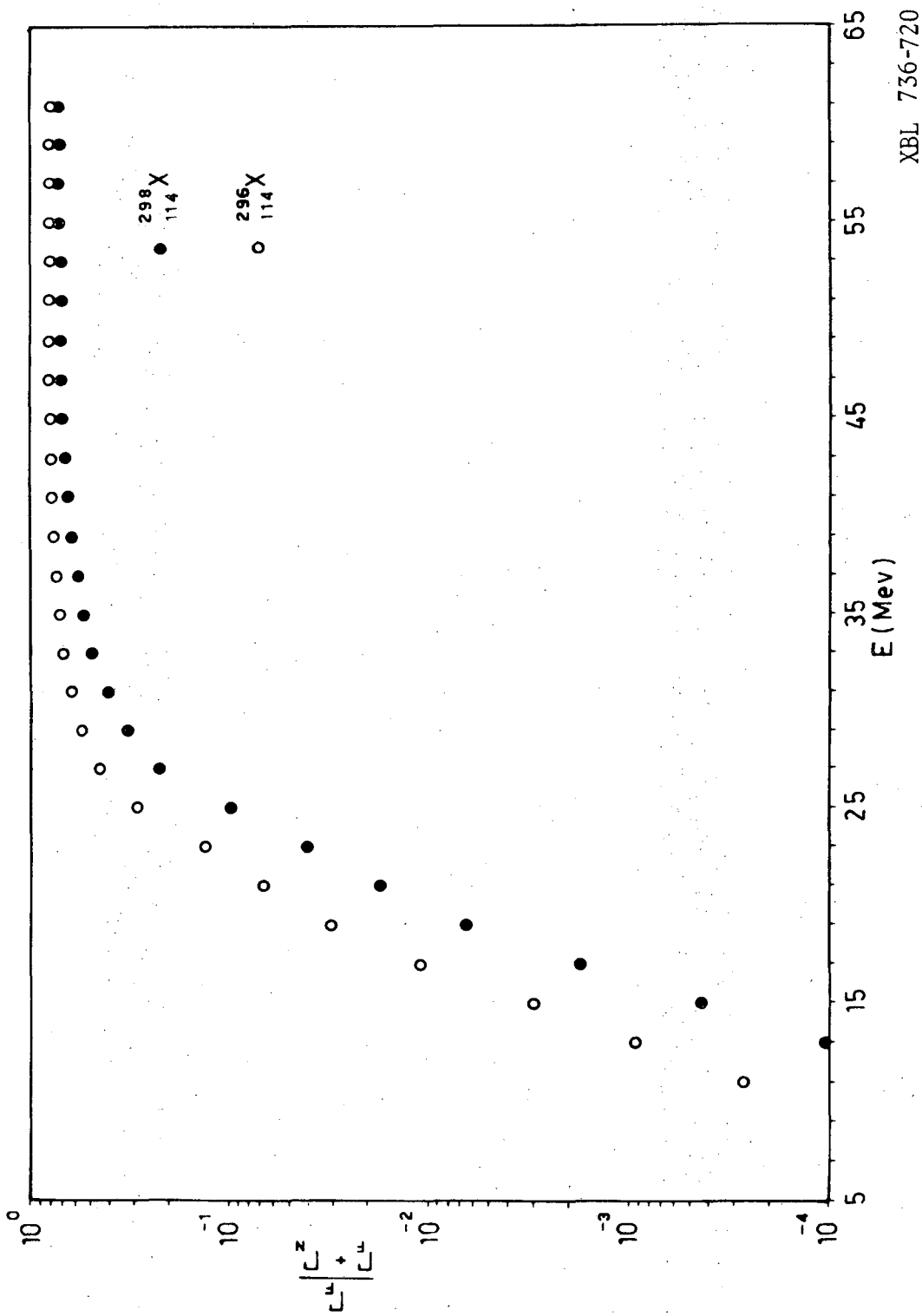
298
114
296
114
E (Mev)
5
15
25
35
45
55
65
10^0
10^{-1}
10^{-2}
10^{-3}
10^{-4}
$\frac{J^N + J^F}{J^F}$
XBL 736-720

Fig. 8b

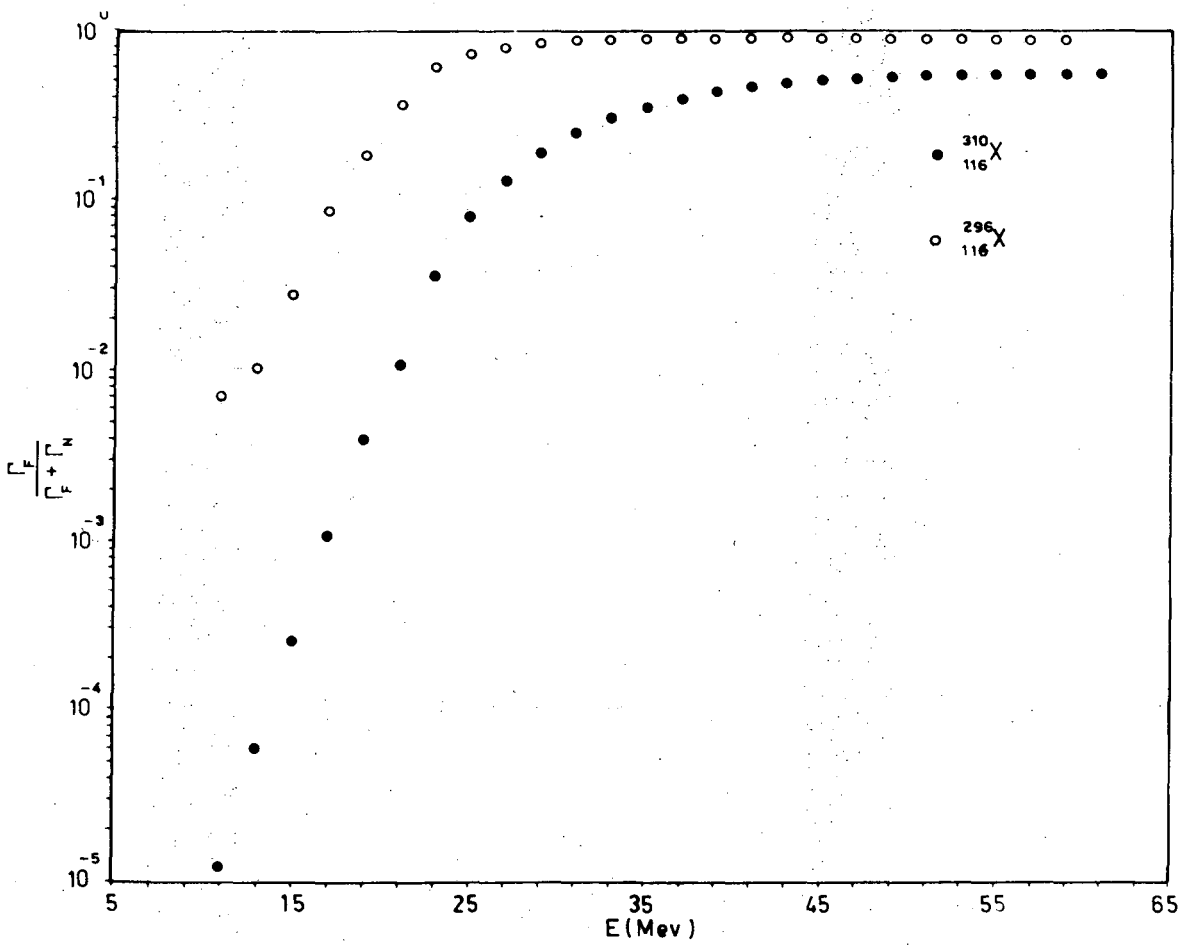

XBL 736-716

Fig. 8c

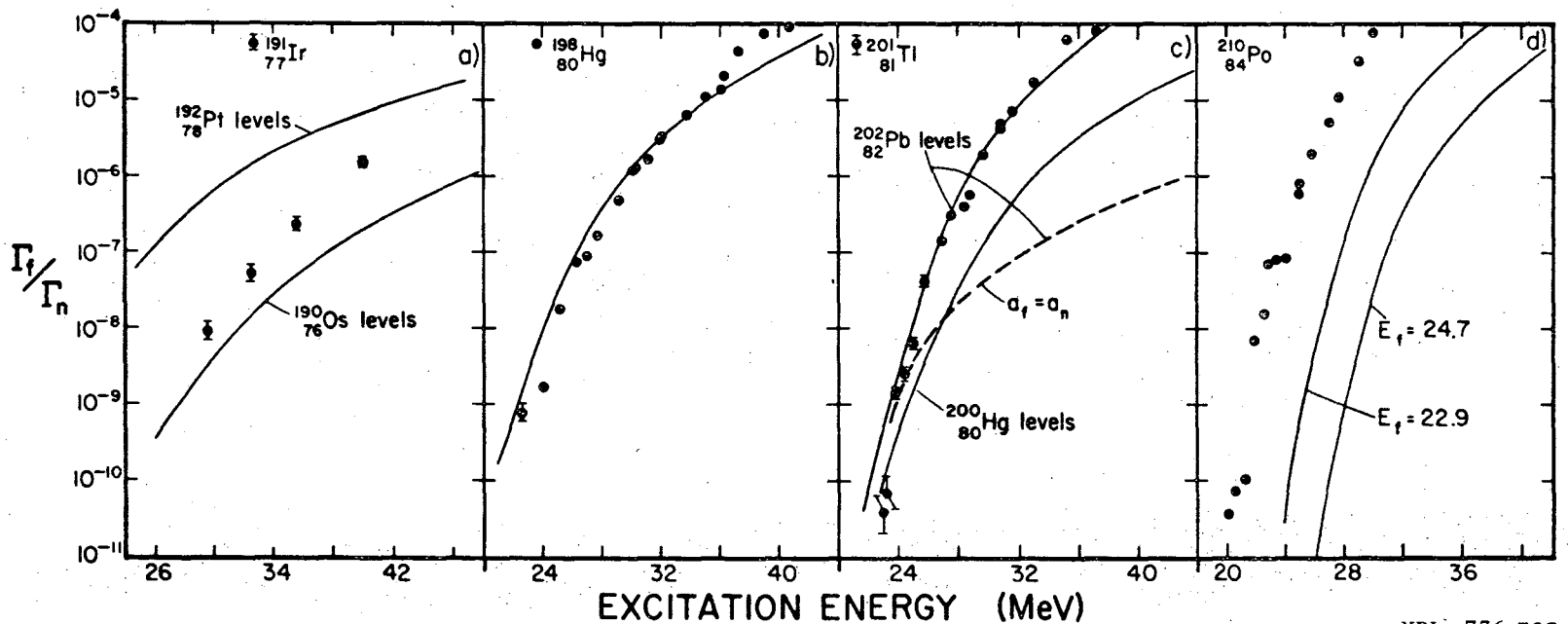

XBL 736-723

Fig. 9

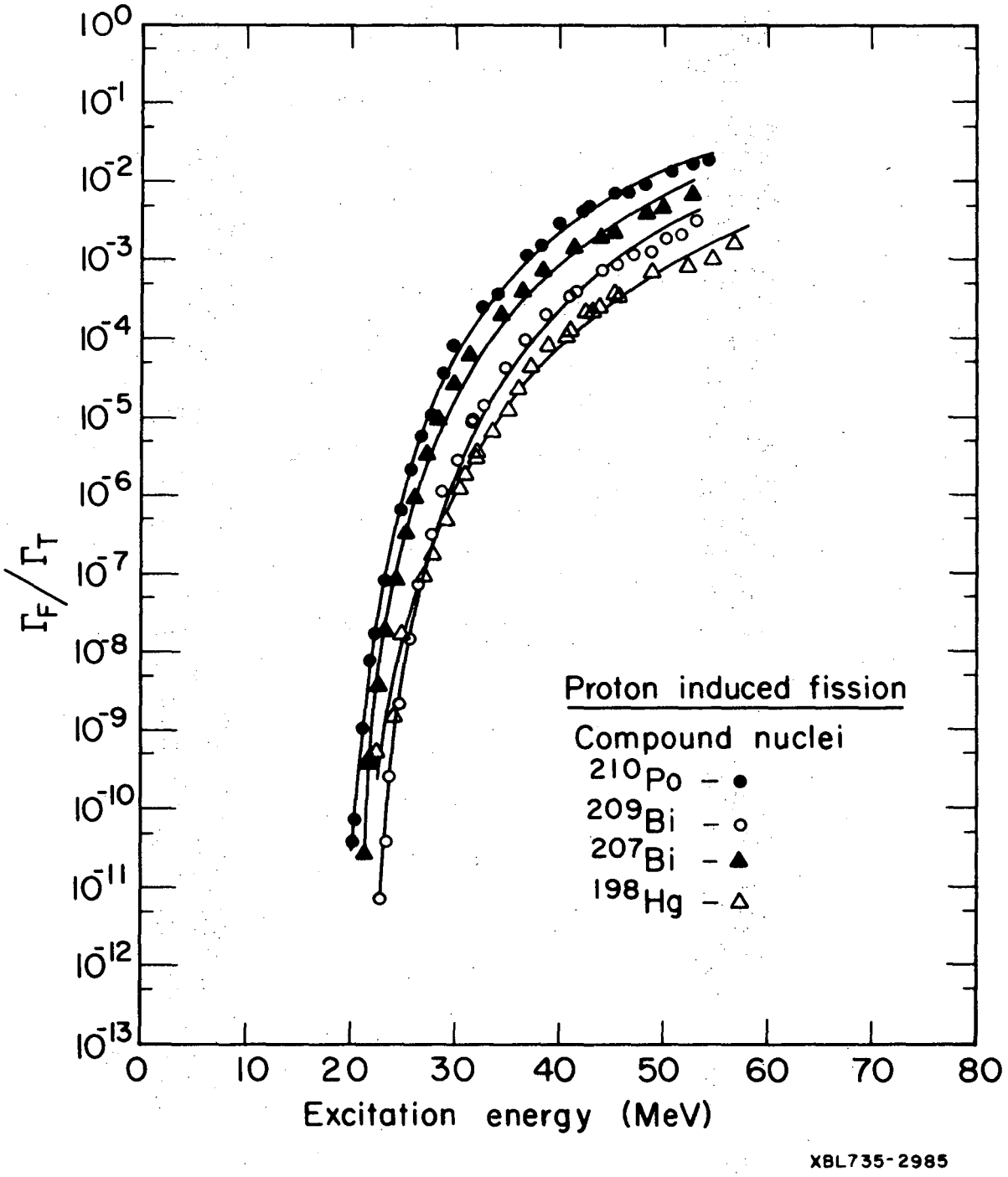
10^0
10^{-1}
10^{-2}
10^{-3}
10^{-4}
10^{-5}
10^{-6}
10^{-7}
10^{-8}
10^{-9}
10^{-10}
10^{-11}
10^{-12}
10^{-13}
Γ_F / Γ_T
0
10
20
30
40
50
60
70
80
Excitation energy (MeV)
Proton induced fission
Compound nuclei
^{210}Po – ●
^{209}Bi – ○
^{207}Bi – ▲
^{198}Hg – △
XBL735-2985

Fig. 10

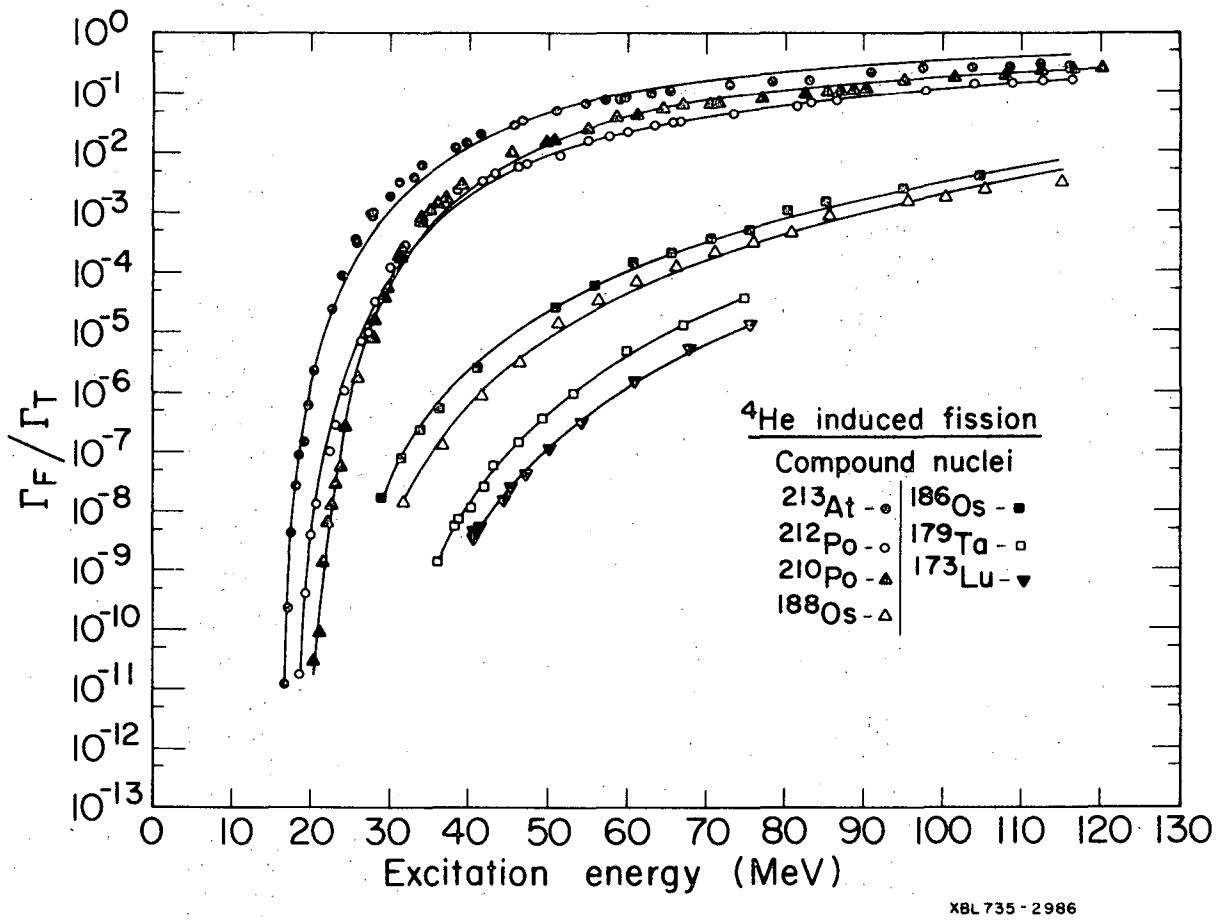
10^0
10^{-1}
10^{-2}
10^{-3}
10^{-4}
10^{-5}
10^{-6}
10^{-7}
10^{-8}
10^{-9}
10^{-10}
10^{-11}
10^{-12}
10^{-13}
Γ_F/Γ_T
0 10 20 30 40 50 60 70 80 90 100 110 120 130
Excitation energy (MeV)
^{4}He induced fission
Compound nuclei
^{213}At - ⊙
^{212}Po - ○
^{210}Po - ▲
^{188}Os - △
^{186}Os - ■
^{179}Ta - □
^{173}Lu - ▼
XBL 735-2986

Fig. 11

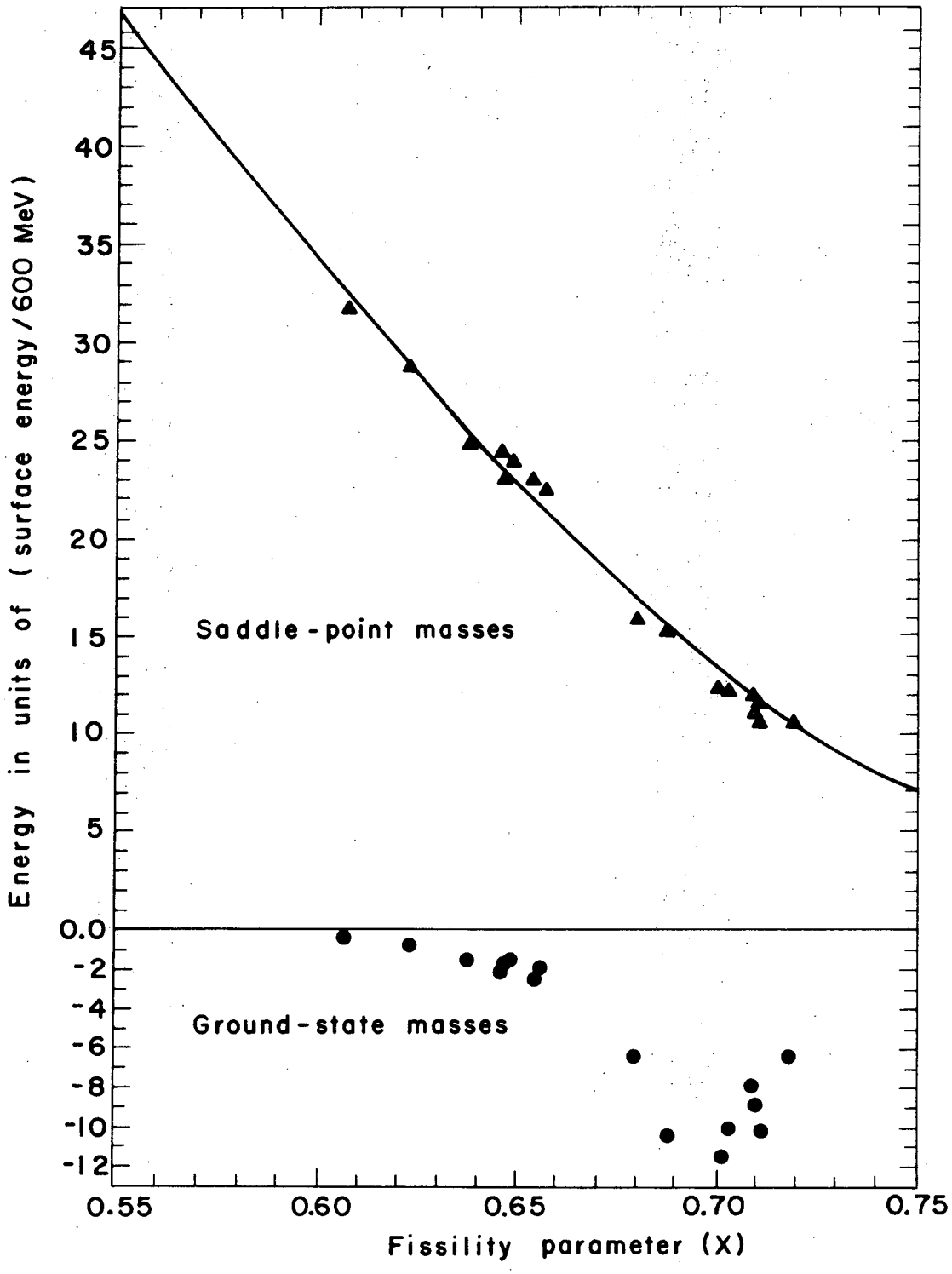

XBL 721-16

Fig. 12

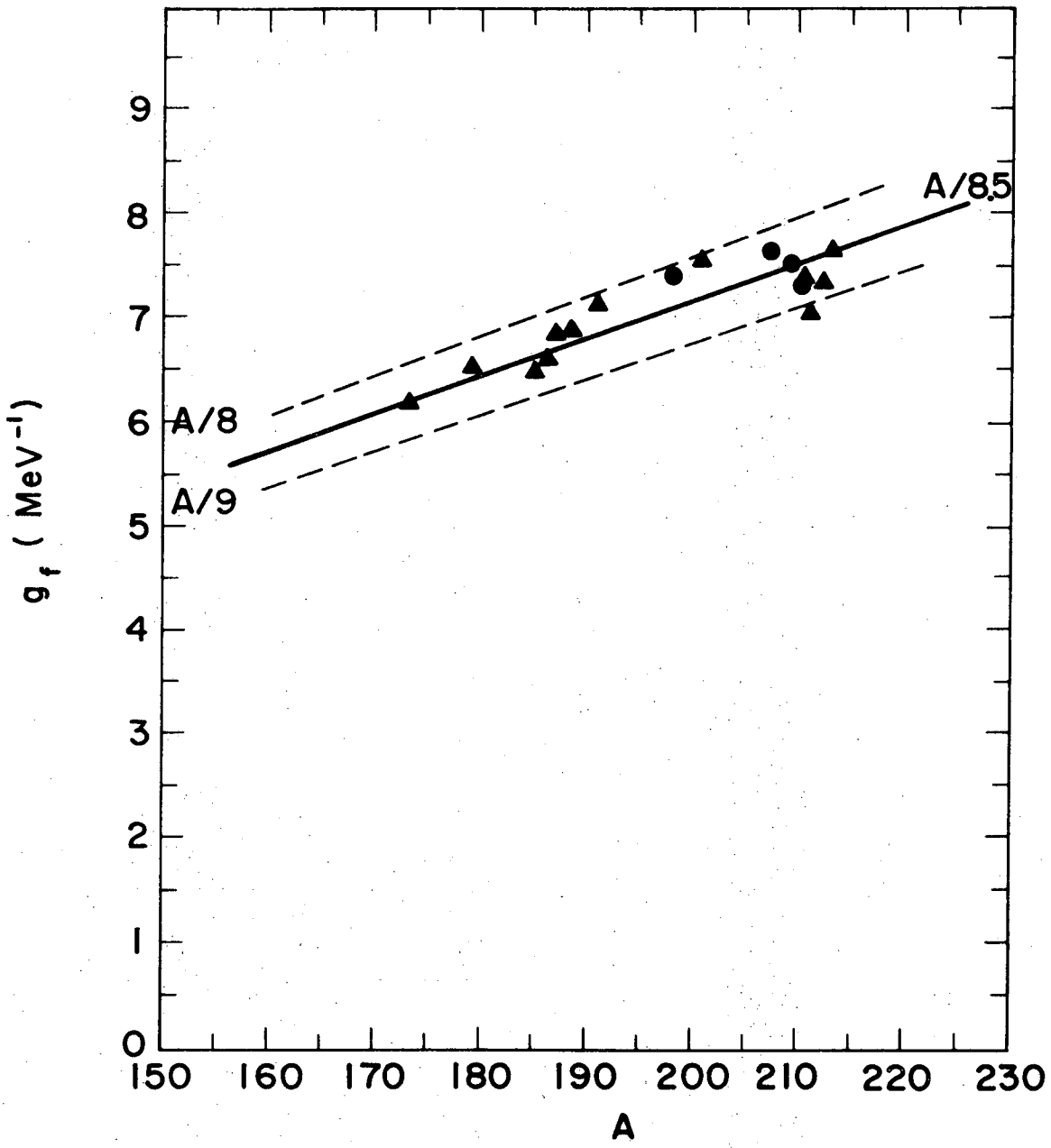

XBL 721-14

Fig. 13

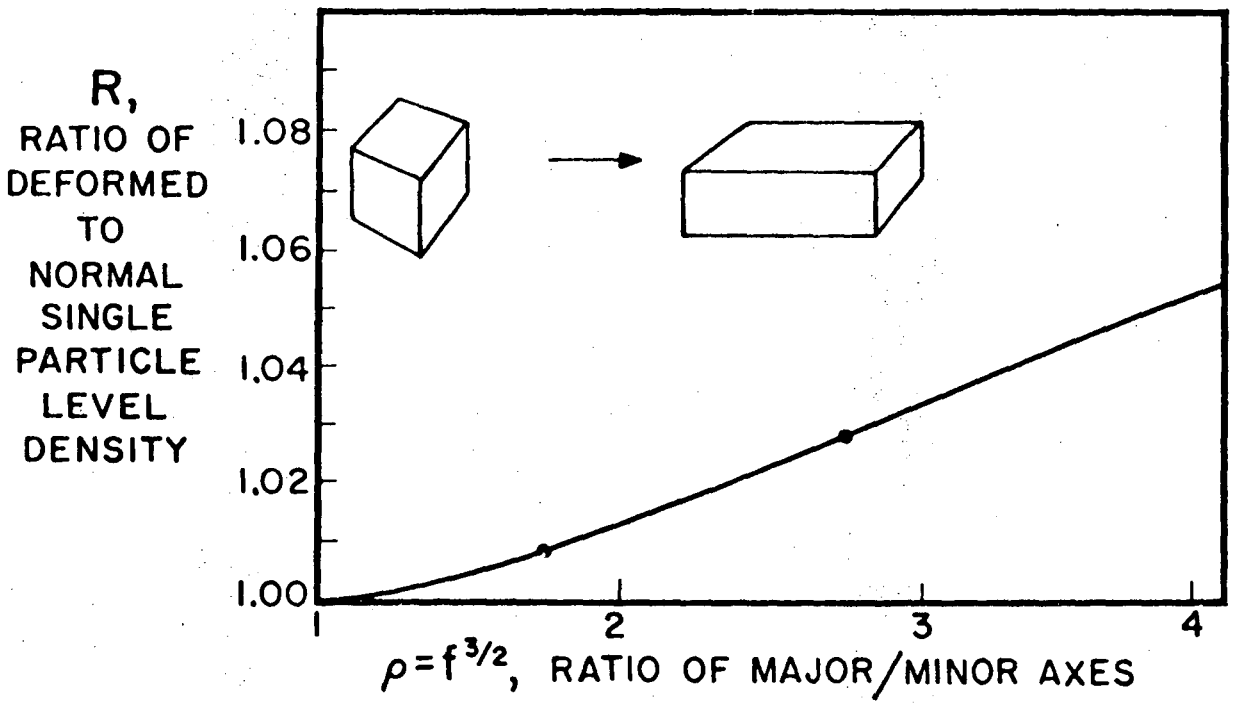

XBL 736-724

Fig. 14

LEGAL NOTICE

This report was prepared as an account of work sponsored by the United States Government. Neither the United States nor the United States Atomic Energy Commission, nor any of their employees, nor any of their contractors, subcontractors, or their employees, makes any warranty, express or implied, or assumes any legal liability or responsibility for the accuracy, completeness or usefulness of any information, apparatus, product or process disclosed, or represents that its use would not infringe privately owned rights.

TECHNICAL INFORMATION DIVISION
LAWRENCE BERKELEY LABORATORY
UNIVERSITY OF CALIFORNIA
BERKELEY, CALIFORNIA 94720